ORIGINAL ARTICLE

Negative CO$_2$ emissions in the lime production using an indirectly heated carbonate looping process

Martin Greco-Coppi[1] · Carina Hofmann[1] · Diethelm Walter[2] · Jochen Ströhle[1] · Bernd Epple[1]

Abstract

Lime is an essential raw material for iron and steel production, in construction and agriculture, in civil engineering, in environmental protection, and in manifold chemical manufacturing processes. To address the problem of unavoidable process CO$_2$ emissions associated with the production of lime, efficient capture technologies need to be developed and implemented. The indirectly heated carbonate looping (IHCaL) process is an efficient candidate for this application because it utilizes lime as the sorbent for the CO$_2$ capture. In this work, a retrofit configuration of this process is presented and analyzed for net negative CO$_2$ emissions. This is done considering different fuels that provide the heat required for the regeneration of the sorbent. The different scenarios were simulated with an AspenPlus® model, key performance indicators were calculated, and the process was compared with other post-combustion capture methods. The results show that net negative CO$_2$ emissions as high as -1805 kg$_{CO2}$/t$_{CaO}$, calculated with a state-of-the-art coal power plant energy scenario ($\eta_e = 44.2$ %; $e_{ref,el} = 770$ kg$_{CO2}$/MWh$_{el}$), can be obtained. This represents an equivalent CO$_2$ avoidance of more than 230% with respect to the reference plant without capture (1368 kg$_{CO2}$/t$_{CaO}$). A specific primary energy consumption for CO$_2$ avoided (*SPECCA*) lower than 1.5 MJ$_{LHV}$/kg$_{CO2,av}$ was achieved for the same energy scenario. Particularly promising results can be accomplished when applying fuels with high biogenic fraction and low specific CO$_2$ emissions, such as solid recovered fuels (SRFs) with a high calorific value.

Nomenclature

AFR	Air-fuel ratio (kg$_{air}$/kg$_{fuel}$)
c_p	Specific heat capacity (massic) (J kg^{-1} K^{-1})
$\bar{c}_p$	Specific heat capacity (molar) (J mol^{-1} K^{-1})
e_{CO2}	CO$_2$ emissions (direct) (kg$_{CO2}$/t$_{CaO}$)
$e_{CO2,fuel}$	Specific CO$_2$ emissions of the fuel (g$_{CO2}$/MJ$_{LHV}$)
$e_{ref,el}$	Reference CO$_2$ emissions for power production (kg$_{CO2}$/MW$_{el}$)
E	Carbon capture efficiency (%)

Extended author information available on the last page of the article

E_{calc}	Calciner efficiency (%)
E_{carb}	Carbonator efficiency (%)
F_0	Molar flow rate of make-up calcium species (kmol/s)
F_{CO2}	Molar flow rate of CO_2 at carbonator inlet (kmol/s)
F_{CO2}^{calc}	Molar flow rate of CO_2 at calciner outlet (kmol/s)
F_{CO2}^{carb}	Molar flow rate of CO_2 at carbonator outlet (kmol/s)
F_R	Molar flow rate of calcium species at carbonator inlet (kmol/s)
h	Height (m)
HHV	Higher heating value (kJ/kg)
HR	Specific heat ratio (-)
HR_a	Absolute heat ratio (-)
LHV	Lower heating value (kJ/kg)
M	Molar mass, atomic mass (kg/kmol)
$\dot{m}_{CaO,prod}$	Total lime production (t/day)
P_{el}	Net power consumption of the entire facility (MW_{el})
PR	Product ratio (-)
q	Fuel consumption (direct) (MJ/t_{CaO})
$\dot{Q}$	Heat flow (MW_{th})
$SPECCA$	Specific primary energy consumption for CO_2 avoided ($MJ_{LHV}/kg_{CO2,av}$)
$T_{preheat}$	Combustor preheated air temperature (°C)
$T_{sorb,calc,in}$	Sorbent temperature at calciner inlet (°C)
x_{bio}	Biogenic carbon fraction in the fuel (%)
X_{bN}	Maximum CaO conversion in the kinetic region after N cycles (mol_{CaCO3}/mol_{Ca})
X_{carb}	Fraction of $CaCO_3$ in the solid stream leaving the carbonator (mol_{CaCO3}/mol_{Ca})
X_{calc}	Fraction of $CaCO_3$ in the solid stream leaving the calciner (mol_{CaCO3}/mol_{Ca})

Greek symbols

Δp	Pressure drop in reactor and auxiliary components (mbar)
η_{h2p}	Heat-to-power efficiency (%)
$\eta_{ref,el}$	Reference electrical efficiency (%)
λ	Air-fuel equivalence rate (-)
Λ	Specific make-up rate (mol_{CaCO3}/mol_{CO2})
τ	Mean residence time or space time (s)
Φ	Specific sorbent circulation rate (mol_{Ca}/mol_{CO2})

Subscripts and superscripts

av	Avoided
bio	Biogenic
calc	Calciner
carb	Carbonator
capt	Captured CO_2
CC	Retrofitted case with carbon capture
comb	Combustor
dry	Dry basis

el	Electric
eq	Equivalent
equil	Equilibrium
FA	Fluidization agent
foss	Fossil
i	Indirect
in	Input, requirement
out	Output, generation
preheat	Combustor preheated air
plant	Reference plant, upstream from capture facility
ref	Reference plant without carbon capture
sorb	Sorbent (CaO and $CaCO_3$)
th	Thermal
wet	Wet basis

Abbreviations

BECCS	Bioenergy with carbon capture and storage
BFB	Bubbling fluidized bed
CaL	Carbonate looping
CCS	Carbon capture and storage
CDR	Carbon dioxide removal
CEN	European Committee of Standardization
CFB	Circulating fluidized bed
CPU	CO_2 compression and purification unit
Cyc.	Cyclone
GHG	Greenhouse gas
HX	Heat exchanger
IHCaL	Indirectly heated carbonate looping
IPCC	Intergovernmental panel on climate change
KPI	Key performance indicator
MSW	Municipal solid waste
PRK	Preheated rotary kiln
RDF	Refuse-derived fuel
Ref	Reference lime production facility without carbon capture
SRF	Solid recovered fuel

1 Introduction

The latest report of the Intergovernmental Panel on Climate Change (IPCC) stated that carbon dioxide removal (CDR) needs to be deployed to achieve net zero greenhouse gas (GHG) emissions (IPCC, 2022). Furthermore, CDR is required in order to cap the global warming to 1.5 °C with no or limited overshoot (IPCC, 2018). CDR is a "key element" to limit global warming because it is the only means to counterbalance the so-called "residual emissions," i.e., uneconomical to abate anthropogenic GHG emissions (Quader and Ahmed, 2017). Emission scenarios compatible with the 1.5 °C limit (67% probability) require huge amounts of CDR on top of deep emissions reductions; namely, 730 Gt_{CO2} on average (IPCC, 2018; Merk et al., 2022). One of the most promising ways to achieve net

negative CO_2 emissions, i.e., CDR, is the implementation of carbon capture and storage (CCS) into industrial processes which emit high amounts of biogenic CO_2 (Clarke et al., 2014; Fuss et al., 2018; Fuss et al., 2014; Quader and Ahmed, 2017). This approach is called bioenergy with carbon capture and storage (BECCS).

Waste-derived fuels have the potential to allow for more economical carbon capture systems due to their lower costs and at the same time enable CDR through BECCS (Haaf et al., 2020c). Refuse-derived fuels (RDFs) and solid recovered fuels (SRFs) are obtained by factions of municipal solid waste (MSW) that cannot be recycled. SRFs are fuels obtained from MSW, which comply with standards from the European Committee for Standardization (CEN) (Gerassimidou et al., 2020), e.g., DIN EN ISO (2021). The term RDF normally refers to waste-derived combustibles of high heating value[1], obtained through the selection of high-quality waste fractions (e.g., paper, wood, plastic, cardboard), which are not defined by CEN standards (Velis et al., 2010). Depending on the quality, consumers may have to pay for these fuels. For low-quality RDF/SRF, suppliers pay the consumers (Sarc and Lorber, 2013).

Lime plants are responsible for the production of raw materials that are widely used in agriculture and the industrial sector. Lime-related products are obtained from the calcination of limestone —mainly calcium carbonate ($CaCO_3$)— at high temperature (900–1200 °C). The calcination reaction is highly endothermic; thus, a heat input is required, e.g., from the combustion of fuels such as coal, coke, and secondary fuels. Carbon dioxide is emitted as a result of the combustion. Additional CO_2 is produced due to the chemical conversion of $CaCO_3$ into calcium oxide (CaO) during the calcination. This so-called "process CO_2," which can only be avoided through CO_2 capture, represents approximately 65 % of the total CO_2 emissions (IEA, 2020a). Overall, the total CO_2 emissions per ton of burnt lime vary between 1 to 2 t_{CO2}/t_{lime} (Schorcht et al., 2013).

In order to capture the process and fuel CO_2 emissions, two groups of carbon capture technologies can be deployed, namely, post-combustion and oxyfuel combustion technologies (Plaza et al., 2020). Only few studies have analyzed carbon capture technologies specifically for the lime industry (Erans et al., 2016; Eriksson et al., 2014; Jafarian et al., 2022; Yang et al., 2020), whereas many works have been published recently that consider carbon capture for the cement industry (e.g., Busch et al., 2022; Nhuchhen et al., 2022; Carbone et al., 2022). There are similarities between both industries, like the calcination of $CaCO_3$, which is the main process in terms of energy consumption (Schorcht et al., 2013). Moreover, CO_2 capture —in particular post-combustion capture— from cement and lime plants have many common features. In both production processes, the majority of the CO_2 emissions come from the raw material, and the specific CO_2 emissions per unit of product are approximately the same. The other components of the flue gas (e.g., HCl, SO_2, moisture, NO_x and N_2, and residual dust) are also comparable if the same fuels are used [2]. A robust process is needed in both cases to capture the CO_2 from the flue gases. Even though this work focusses on the CO_2 capture from a lime plant, reference studies on carbon capture from cement kilns are used for comparison purposes.

Eriksson et al. (2014) proposed using oxyfuel combustion directly in a lime rotary kiln. They found that, with this system, the total CO_2 emissions may be reduced, but pointed out the technical challenges to control the temperature and, in this way, comply with the high-quality standards of rotary kiln lime products. The environmental

---

[1] Typically, *LHV$_{wet}$* ranges from 14 to 20 MJ/kg for these fuels (Bhatt et al. 2021).

[2] Reference values can be found in Schorcht et al. (2013).

and economic potential of oxyfuel combustion for cement production was analyzed by different authors (e.g., Rolfe et al., 2018; Barker et al., 2009). Carrasco et al. (2019) investigated oxyfuel carbon capture from the cement production in a 500 kW$_{th}$ testing facility. This technology has good energy performance, but presents significant disadvantages when it comes to retrofitability (Voldsund et al., 2019b).

Post-combustion CO_2 capture technologies have a high CO_2 abatement potential and are more suitable for retrofitting compared to oxyfuel combustion (Voldsund et al., 2019b). Nonetheless, the majority of these technologies have very high energy requirements, which increase the costs of the final products and reduce the efficiency of the entire system considerably. Gardarsdottir et al. (2019) evaluated different post-combustion carbon capture processes for the cement production. They calculated that monoethanolamine-based absorption, the reference post-combustion carbon capture technology, has a specific primary energy consumption for CO_2 avoided (*SPECCA*) of 7.02 MJ/kg$_{CO2,av}$ and a cost of CO_2 avoided of 80.2 €/t$_{CO2,av}$. Barker et al. (2009) estimated that the cost of CO_2 avoided would be higher than 100 €/t$_{CO2,av}$ to retrofit a 1 Mt$_{cement}$/y cement plant located in North East Scotland with a solvent-based post-combustion capture unit.

One noteworthy post-combustion carbon capture technology is the carbonate looping (CaL) process (Shimizu et al., 1999), whereby the CO_2 capture is achieved by utilizing limestone as a sorbent, i.e., the raw material of the lime production facility. The sorbent binds CO_2 from the kiln flue gases in a carbonator and is regenerated through a temperature increase in a calciner, according to the reaction in Eq. (1) (Anantharaman et al., 2018).

$$CaCO_{3(s)} \rightleftharpoons CO_{2(g)} + CaO_{(s)}; \Delta H_{298K} = \pm 1,780 \text{kJ/kg} \tag{1}$$
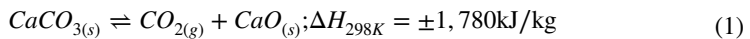
For the regeneration of the sorbent in the standard CaL process, fuel is burnt directly in the calciner. For this, technically pure oxygen is used, which requires an air separation unit (ASU) (Carrasco-Maldonado et al., 2016). CaL technology has the potential to efficiently capture CO_2 from lime plants by exploiting the synergies of the calcination.

The CaL process has been successfully operated up to the pilot scale in Stuttgart, Germany (200 MW$_{th}$) (Charitos et al., 2011; Dieter et al., 2014; Hornberger et al., 2021, 2020), in Darmstadt, Germany (1 MW$_{th}$) (Haaf et al., 2020b; Hilz et al., 2018, 2017; Kremer et al., 2013; Ströhle et al., 2020; Ströhle et al., 2014), and in La Pereda, Spain (1.7 MW$_{th}$) (Arias et al., 2017b; Arias et al., 2013; Diego et al., 2020; Diego et al., 2016b). For power plants, the CaL process has the potential to achieve high CO_2 capture rates with low energy penalties. Lasheras et al. (2011) estimated that a full-scale power plant could be retrofitted with CaL to capture 88% of the total CO_2 formed, with an energy penalty of less than 2.9%. Astolfi et al. (2019) calculated that a *SPECCA* of 2.16 MJ$_{LHV}$/kg$_{CO2,av}$ could be achieved by the integration of the CaL process into power plants with thermochemical energy storage, and Haaf et al. (2020a) estimated a *SPECCA* of 5.72 MJ$_{LHV}$/kg$_{CO2,av}$ for the integration into waste-to-energy plants.

Experimental investigations are being carried out to apply CaL technology into the cement industry. Arias et al. (2017a) achieved more than 90% CO_2 capture in a CaL 30 kW$_{th}$ test facility at relevant conditions for cement plants. Within the CLEANKER project, a demonstrator CaL unit has been erected to capture CO_2 from an operating cement plant that produces 1.3 Mt$_{cement}$/y in Vernasca, Italy (Fantini et al., 2021). De Lena et al. (2022) investigated the application of different CaL configurations into the cement industry and reported *SPECCA* values between 2.8 and 3.0 MJ$_{LHV}$/kg$_{CO2,av}$ for systems utilizing pure limestone as sorbent, and between 3.5 and 4.6 MJ$_{LHV}$/kg$_{CO2,av}$ for systems that utilize cement raw meal.

The ASU in the CaL process increases the *SPECCA* by approximately 1 MJ_{LHV}/ $kg_{CO2,av}$ (De Lena et al., 2022). The requirement for technically pure O_2 can be avoided by indirectly heating the calciner, e.g., through solid looping (Diego et al., 2016a), and thus the energy penalty is reduced (Martínez et al., 2016). One excellent means to achieve this is through heat pipes (Hoeftberger and Karl, 2016), which transfer heat from an external combustor into the calciner via evaporation and condensation of a fluid. This indirectly heated carbonate looping (IHCaL) process (Epple, 2009) presents several advantages compared to the oxy-fired CaL process: reduced energy requirement, improved sorbent activity, lower sorbent attrition rates, and high purity of the captured CO_2. It has the potential to enable carbon capture with very low CO_2 avoidance costs[3] (Junk et al., 2016).

The IHCaL process has been successfully operated for 400 h at the 300 kW_{th} facility of the Technical University of Darmstadt (Reitz et al., 2016) in operating conditions corresponding to CO_2 capture from coal-fired power plants. Additional test campaigns in Darmstadt were carried out during 2022 to prove the operability of the IHCaL process under lime plant conditions at the pilot scale with solid fuel feedstock (Hofmann et al., 2022a, 2022b; Ströhle et al., 2021). The facility was operated for more than 300 additional hours during the year 2022.

Furthermore, the utilization of secondary fuels has been successfully demonstrated up to the pilot scale (1 MW_{th}) for CaL operation (Haaf et al., 2020d; Haaf et al., 2020b). Regarding the IHCaL process, different solid fuels were fueled in the 300 kW_{th} heat pipe IHCaL testing facility of the Technical University of Darmstadt (Hofmann et al., 2022a, 2022b). The combustor was operated around 20 h with lignite and around 20 h with RDF pellets, with the compositions and heating values displayed in Table 5.

At the Technical University of Darmstadt, novel concepts for the integration of the IHCaL process into the lime production were developed and evaluated through process simulation (Greco-Coppi et al., 2021). The published results show that the direct CO_2 emissions can be reduced by up to 87% by utilizing dried lignite as fuel for both the lime kiln and the IHCaL combustor. Nevertheless, the application of waste-derived fuels into these concepts to enable CDR has not been discussed yet.

This work investigates the influence of four different fuels on the CO_2 emissions and energy requirements of a tail-end IHCaL process integrated into a lime plant. The objective of this paper is to unravel the potential of the IHCaL process to achieve net negative CO_2 emissions, thus enabling CDR. Furthermore, it aims to assess the energy performance of the IHCaL process, compared to other carbon capture technologies that are being considered for deployment in the cement and lime industries.

2 Methodology

2.1 Process integration

The IHCaL concept considered in this paper is referred to as the tail-end or retrofit configuration in previous works reported in the literature (Greco-Coppi et al., 2021; Junk et al.,

---

[3] Junk et al. (2016) reported 22.6 €/$t_{CO2,av}$ for an IHCaL process (without compression) integrated into a 1052 MW_{el} hard-coal-fired power plant.
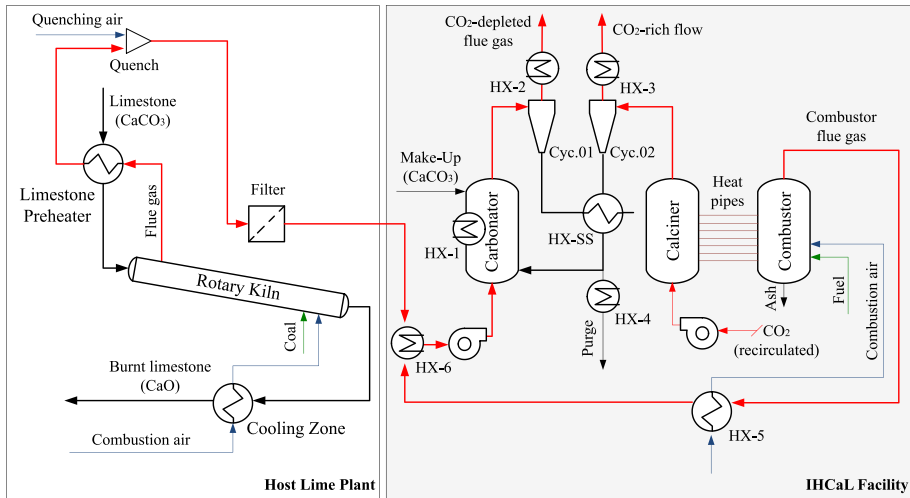
Fig. 1 Tail-end concept for the integration of the IHCaL CO_2 capture process into an existing lime plant, introduced by Greco-Coppi et al. (2021)

2013). This process is suitable for capturing CO_2 from operating lime plants[4]. The configuration is shown schematically in Fig. 1. It consists of a host lime plant (left side) and an IHCaL facility (right side). In Europe, this configuration has the potential to decarbonize existing facilities with more than one kiln. The IHCaL facility replaces one kiln and, at the same time, captures the CO_2 of the remaining kilns.

The host facility for this work is the lime production line located in Germany described by Greco-Coppi et al. (2021). The rotary kiln is equipped with a limestone preheater (PRK) and is fueled with dried lignite ($LHV = 21500$ kJ/kg$_{wet}$). The burnt lime (mainly CaO) is cooled downstream of the kiln with the combustion air. The kiln flue gases are used to preheat the raw material. An air quench is used to reduce the temperature before the filter and the blower. The flue gases exit the host plant at 236 °C and high[5] CO_2 concentrations (19.0 vol%$_{dry}$).

The IHCaL facility allows for the capture of CO_2 utilizing CaO as sorbent and increases the total production of the plant through the calcination of the make-up stream ($CaCO_3$). There are three main reactors: (i) a carbonator operating as a circulating fluidized bed (CFB) for the absorption of CO_2, (ii) a calciner operating in a bubbling bed regime (BFB) for the sorbent regeneration, and (iii) a BFB combustor providing the energy required to regenerate the sorbent.

The flue gases from the kiln and the combustor are cooled at HX-6 to reduce the propelling energy requirements. Afterwards, they enter the carbonator from the bottom by means of a blower. The same flue gas is the fluidizing agent that allows for

---

[4] Greco-Coppi et al. (2021) showed that the fully integrated IHCaL process would be more suitable for newly built CO_2 lime plants, compared to the tail-end concept, when utilizing dried lignite to fuel the combustor.

[5] Previous pilot tests on the 300 kW$_{th}$ IHCaL pilot facility in Darmstadt demonstrated the feasibility to capture CO_2 from more diluted flue gas (14 vol%$_{dry}$), corresponding to typical power plant flue gases (Reitz et al. (2014); Reitz et al. (2016)).

the CFB operation. In the carbonator, the CO_2 from the flue gas is absorbed by the circulating sorbent (CaO) to form $CaCO_3$. The CO_2-depleted flue gas exits the IHCaL facility through the cyclone 1, and the $CaCO_3$ enters the calciner. In the calciner, the sorbent is regenerated, and the CO_2 is released in a high concentration (> 95 vol%$_{dry}$) stream. This CO_2 is then conditioned for transport and storage. The main assumptions for the downstream conditioning facility are presented in Section 2.3. The solids leaving the calciner enter the carbonator; thus, the calcium loop is established. Heat is supplied into the calciner from the combustor via heat pipes (Hoeftberger and Karl, 2016). The combustor can be fueled with lignite or waste-derived fuels, as explained in Section 2.5.

As a result of the deactivation of the sorbent, a constant make-up is required to maintain a high carbon capture rate (Grasa and Abanades, 2006). Make-up can be added into the process directly into the carbonator or the calciner or into the connecting elements (e.g., loop seals). The used sorbent (CaO) is removed from the system downstream of the calciner and may be sold as burnt lime[6]. The limestone composition from the host lime plant (see Table 1) is considered in this work. It is assumed that this limestone is used, not only for the rotary kiln, but also as make-up and sorbent for the IHCaL process.

2.2 Process model

The heat and mass balances were calculated with the software AspenPlus®, version V12. Custom routines in FORTRAN code were included. Steady-state conditions were assumed, and the cyclone separation was considered ideal. The ambient pressure and temperature were set to 1.013 bar and 15 °C, respectively, and a plant capacity factor of 91.3% was assumed in accordance with Voldsund et al. (2019a). The calculation of the material properties and the balances in the reactors was performed as explained by Greco-Coppi et al. (2021). For the combustor, an air-fuel equivalence ratio (λ) of 1.2 was specified.

The temperatures of the reactors and the main operating parameters for the calculations are displayed in Table 2. It was assumed that the reactors, heat exchangers, and ducts are adequately insulated, and thus the thermal losses are negligible. Accordingly, these components were modeled adiabatic (Chen et al., 2020).

In this work, the make-up solid stream (F_0) and the circulating solid stream (F_R) are calculated from defined ratios (Λ, Φ) and the total CO_2 molar flow rate entering the carbonator (F_{CO2}), according to Eq. (2).

$$F_0 = \Lambda \cdot F_{CO2}; \ F_R = \Phi \cdot F_{CO2} \tag{2}$$

The CO_2 capture efficiency (E, see Eq. 7), is given as an input: $E = 90\%$. The required carbonator efficiency (E_{carb}) is calculated with Eq. (3), from the molar flow rates of CO_2 entering (F_{CO2}) and leaving (F_{CO2}^{carb}) the carbonator.

---

[6] The suitability of the spent sorbent to be sold as burnt lime is still being investigated. Some previous studies (Dean et al. 2013; Hills 2016) suggest that this is possible. Within the ANICA project, the spent sorbent of the pilot testing campaigns at the Technical University of Darmstadt will be tested to verify its quality compared to the rotary kiln product (Ströhle et al. 2021).

Table 1 Composition of the limestone used in the reference plant and in the IHCaL carbon capture facility (Greco-Coppi et al., 2021)

Component	Mass fraction
$CaCO_3$	98.3%
$MgCO_3$	0.7%
SiO_2	0.7%
Fe_2O_3	0.1%
Al_2O_3	0.2%
SO_3	< 0.1%

Table 2 Main operating parameters of the IHCaL process

Parameter	Value
Main IHCaL parameters	
CO_2 capture efficiency (E)	90%
Calciner efficiency (E_{calc})	99%
Specific sorbent circulation rate (Φ)	(variable)
Specific make-up rate (Λ)	$0.10\,\text{mol}_{CaCO3}/\text{mol}_{CO2}$
Operating temperatures	
Carbonator (T_{carb})	650 °C
Calciner (T_{calc})	900 °C
Combustor (T_{comb})	1000 °C
Combustion air preheating, after HX-5 ($T_{preheat}$)	800 °C
Sorbent at calciner inlet, after HX-SS ($T_{sorb,calc,in}$)	810 °C

$$E_{carb} = 1 - \frac{F_{CO2}^{carb}}{F_{CO2}} \tag{3}$$

The calciner efficiency is an input for the model and is defined as:

$$E_{calc} \equiv \frac{X_{carb} - X_{calc}}{X_{carb}} \tag{4}$$

Here, X_{calc} and X_{carb} are the fractions of $CaCO_3$ in the calcium (Ca) stream leaving the calciner and the carbonator, respectively. The composition of Table 1 was used to model the limestone streams. This includes the make-up stream and the raw material input into the rotary kiln.

The carbonator efficiency (E_{carb}) is calculated with the carbonator reactor model developed by Lasheras et al. (2011) that considers: (i) circulating fluidized bed hydrodynamics according to Kunii and Levenspiel (1991); (ii) the carbonation reaction model from Abanades et al. (2004); and (iii) sorbent deactivation as modeled by Abanades et al. (2005). The make-up rate was set to $\Lambda = 0.1$, and Φ was varied to achieve the necessary CO_2 capture efficiency of $E = 90\%$. The carbonator reactor model assumptions and results are included in Appendix 1 and Appendix 2, respectively.

2.3 Power requirements

In this work, the battery limits for the analysis are the input of the flue gases from the reference facility before the stack and the exit from the CO_2 compression unit. The CO_2 emissions and primary energy consumption related with the transport and storage of CO_2, transport and pre-treatment of raw materials and fuels (e.g., fractioning), and the erection of the carbon capture facility are out of the scope of this paper[7]. The main assumptions and input parameters for the analysis are summarized in Table 3.

For the calculation of the electric power in the reference facility, the data from the best available technique reference document for cement, lime, and magnesium oxide (Schorcht et al., 2013) was considered: 17–45 kWh/t_{lime} for a lime rotary kiln. The mean value was used for the calculations: 31 kWh/t_{lime}. The power demand from the IHCaL facility and the downstream conditioning are used to obtain the net power generation (P_{el}) for the calculation of the indirect CO_2 emissions (Eq. 12) and indirect primary energy consumption (Eq. 10).

After a post-combustion carbon capture facility, downstream conditioning of the captured CO_2 is necessary. For oxy-fired CaL, purification is required due to the presence of combustion gases other than CO_2 (mainly O_2). Furthermore, the CO_2 stream is to be compressed up to a suitable temperature for transportation of around 110 bar. Such CO_2 compression and purification units (CPUs) have relatively high energy requirements that range from 80 to 120 kWh$_e$/t_{CO_2} (De Lena et al., 2018; Garðarsdóttir et al., 2018; Jackson and Brodal, 2019; Magli et al., 2022; Svensson et al., 2021). In the IHCaL process presented in this work, the combustion to generate the heat for the regeneration takes place in an external combustor, and thus the CO_2 stream after the calciner is almost pure. The only conditioning required is the cooling and the filtering, after which, the stream is ready for compression. The compression takes place in a 5-stage CO_2 compressor. The compression was simulated in Aspen Plus, based on the method reported by Posch and Haider (2012). The assumptions for the compression unit are reported in Table 3.

The power requirement of the blowers depends on the pressure drop (Δp) in the reactors and the auxiliary components, i.e., the nozzle grid, cyclone, cooler, filter, and ducts. The following values were assumed according to the experimental data of the research group: 100 mbar for the carbonator, 130 mbar for the calciner, and 150 mbar for the combustor (Reitz et al., 2016). For the blowers, the isentropic and mechanical efficiencies were set to 0.65 and 0.9, respectively (Grote and Feldhusen, 2007). It was assumed that the flue gases entering the carbonator and the combustion air act as fluidization agents for the corresponding reactors. For the calciner, the fluidization agent[8] is a fraction of the pure CO_2 flow stream that is recirculated to allow for BFB operation. To calculate the amount of recirculation required, the following assumptions were made: (i) superficial velocity for the

---

[7] Carbone et al. (2022) performed a carbon footprint evaluation on a similar process, namely, an oxy-fired CaL process for cement plants. Their results suggest that the specific CO_2 emissions associated with the infrastructure are similar in plants without carbon capture and with downstream CaL. Furthermore, the contribution of GHG emissions in the supply of the raw meal (sorbent) was almost negligible.

[8] In this work, it is assumed that an external fluidization agent, i.e., recirculated CO_2, is required for the fluidization of the calciner. Hoeftberger and Karl (2013) demonstrated the so-called self-fluidization of the IHCaL calciner experimentally. In the self-fluidization regime, no external fluidization agent is required, because the amount of CO_2 released during the calcination is enough to maintain the fluidization of the BFB. If the calciner were operated without an external fluidization agent, the power requirements would be reduced.

Table 3 Main assumptions and general input parameters for the calculation of power requirements

Parameter	Unit	Value
CO$_2$ Compression		
Number of stages[a]	-	5
Temperature after intercooler	°C	25
Pressure drop intercooler	mbar	100
Polytropic efficiency	%	80
Mechanical efficiency	%	95
Discharge temperature	°C	25
Discharge pressure	bar$_a$	110
Inlet temperature	°C	25
Inlet pressure	bar$_a$	1.013
Blowers of the IHCaL facility		
Mechanical efficiency	%	90
Isentropic efficiency	%	65
Δp_{carb}	mbar	100
Δp_{calc}	mbar	130
Δp_{comb}	mbar	150
$u_{0,calc}$	m/s	0.25
F_{calc}	Nm^3/h	9700
$T_{FA,carb}$	°C	250
$T_{FA,calc}$	°C	450

[a]Equal pressure ratio

fluidization agent at inlet $u_{0,calc} = 0.25$; (ii) heat pipe properties as reported by Höftberger et al. (2016), namely, 3 m calciner width (i.e., 6 m heat pipes), 7.2 m calciner length/50 MW$_{th}$; (iii) and calciner heat input equal to 100 MW$_{th}$. Finally, the temperature of the fluidization agent (T_{FA}) before the blowers is defined. The air for the combustor is compressed from ambient temperature. The flue gases entering the carbonator are cooled down to 250 °C before the compression, and the recirculated gases for the fluidization in the calciner are cooled down to 450 °C.

2.4 Heat integration and power generation

The configuration displayed in Fig. 1 allows for efficient heat utilization. The combustion air for the combustor is preheated ($T_{preheat}$), and heat is exchanged between the solid streams to increase the temperature of the solids entering the calciner ($T_{sorb,calc,in}$). These design specifications minimize the total heat requirement, as shown by Greco-Coppi et al. (2021).

To achieve a high $T_{sorb,calc,in}$, a solid-solid heat exchanger (HX-SS) is required. Different configurations are possible for the design of this heat exchanger: (i) a concept that utilizes molten salt circulating inside of metal tubes; (ii) a concept with heat-pipes, similar to those presented by Hoeftberger and Karl (2016) to transfer heat into the calciner; (iii) a concept with high surface area metal walls separating the solid flows; and (iv) a concept consisting of two concentric L-valves (Greco-Coppi et al., 2021). For the considered inputs (see Table 2), a counter-current configuration of this heat exchanger yields a logarithmic mean temperature difference of around 90 °C.

The high operating temperatures (650–900 °C) make the IHCaL process particularly suitable for power generation through a heat recovery steam cycle (De Lena et al., 2018; Lasheras et al., 2011). Steam can be produced from the cooling of the carbonator and from the gas streams exiting the carbonator (650 °C), the calciner (900 °C), and the combustor (1000 °C). For the calculation of the power generation through a heat recovery steam cycle, the recovered heat is obtained from the AspenPlus® simulations. The temperatures assumed for this purpose are displayed in Table 4.

For the calculation of the power generation, the steam cycle was simulated with the software EBSILON Professional^{TM}. The main assumptions for the calculations were: (i) superheating of steam up to 565 °C and 130 bar; (ii) preheating of feed-water with steam extractions; (iii) isentropic turbine efficiency equal to 85%. The calculated heat-to-power efficiency (η_{h2p}) was 42.4%. This value corresponds to an equivalent net electrical efficiency of around 38% for a thermal power plant (e.g., pulverized coal), which is in agreement with values from the literature (IEA, 2020b). The total power generation from the IHCaL facility can be calculated with Eq. (5). Here, $\dot{Q}_{IHCaL,HRSG}$ is the recovered heat from the IHCaL unit.

$$P_{el,out} = \eta_{h2p} \cdot \dot{Q}_{IHCaL,HRSG} \tag{5}$$

2.5 Fuels and CO_2 emissions

The focus of this work lies on the investigation of the effect of implementing different fuels in the IHCaL process. The biogenic CO_2 capture and associated negative emissions are of special interest. Four fuels were selected for the analysis: (i) dried lignite from the reference process in the host plant in Germany (Greco-Coppi et al., 2021); (ii) RDF pellets, which are used in pilot test campaigns at the Technical University of Darmstadt (Ströhle et al., 2021); (iii) a class 3 SRF, according to EN ISO 21640:2021-11 (2021), that was successfully utilized in the 1 MW$_{th}$ pilot plant at the Technical University of Darmstadt for CaL operation (Haaf et al., 2020d); and (iv) municipal solid waste (MSW), with the composition from the CaL techno-economic analysis from Haaf et al. (2020a). Dried lignite was maintained as the fuel of the reference plant for all cases, and only the fuel for the IHCaL combustor was varied.

The fuel CO_2 emissions index (Furimsky, 2007; Madejski et al., 2022) is also known as the fuel-specific CO_2 emissions, $e_{CO2,fuel}$ (g$_{CO2}$/MJ$_{LHV}$). It indicates the mass of CO_2 produced by the combustion of fuel per unit of energy obtained. The Eq. (6) can be used to calculate it. Here, $w_{c,wet}$

Table 4 Operating temperatures for the heat exchangers (HX), flue gas side

Operating temperatures in heat exchangers (°C)	Upstream	Downstream
HX-1: carbonator[a]	650	-
HX-2: carbonator flue gas	650	250
HX-3: calciner flue gas	900	250
HX-4: purge (for air preheating)[b]	900	40
HX-5: preheater[c]	1000	(Variable)
HX-6: flue gases before carbonator	350	250

[a]No temperature change on the flue gas side due to the carbonation heat of the reaction

[b]Solid stream side

[c]The design temperature is the downstream temperature on the air side ($T_{preheat}$)

is the wet-basis mass fraction of carbon in the fuel, LHV_{wet} is the fuel lower heating value in wet basis, M_{CO2} is the molar mass of CO_2, M_c is the molar mass of carbon. The input parameters of the fuels considered in this analysis, including the CO_2 emissions index, are presented in Table 5.

$$e_{CO2,fuel} = \frac{w_{c,wet}}{LHV_{wet}} \cdot \frac{M_{CO2}}{M_C} \tag{6}$$

For the calculation of the negative CO_2 emissions, the biogenic and fossil emissions are distinguished. CO_2 emissions from pre-dried lignite are considered 100% fossil, as well as the emissions from limestone calcination. For the fuels burnt in the combustor, the biogenic carbon fractions (x_{bio}) are defined. According to Moora et al. (2017), x_{bio} varies considerably depending on the waste selection process and the region-dependent source segregation. The determination of the x_{bio} of the RDF pellets was performed according to the German standard DIN EN 15440:2011 (2011). For the other fuels, x_{bio} was assumed considering values from the literature (Astrup et al., 2009; Haaf et al., 2020a; Mohn et al., 2012; Mohn et al., 2008; Obermoser et al., 2009). Astrup et al. (2009) reported a range of 45–85% for MSW and explained that the biogenic carbon content of SRF is normally low, compared to MSW, because of the selective fractioning. The values of x_{bio} used in this work are displayed in Table 5.

2.6 Key performance indicators

Key performance indicators (KPIs) of the IHCaL process are the carbon capture efficiency (E), the heat ratios (HR_a, HR), and the product ratio (PR). The carbon capture efficiency of the IHCaL process (E) is defined as the ratio of CO_2 captured to total CO_2 generated. It can be calculated as follows:

$$E = \left(1 + \frac{F_{CO2}^{carb}}{F_{CO2}^{calc}}\right)^{-1} \tag{7}$$

Table 5 Input parameters of the fuels used in this analysis

Parameter	Unit	Dried lignite[a]	RDF pellets[b]	SRF[c]	MSW[d]
LHV	MJ/kg$_{wet}$	21.5	19.6	15.7	10.0
x_{bio}	%	0	51	45	60
$e_{CO2,fuel}$	g$_{CO2}$/MJ$_{LHV}$	96.7	92.8	88.7	106.0
Particle size	mm	0–4	ø 5	$d_{95} < 50$	$d_{95} < 100$[e]
C	wt.%$_{wet}$	56.7	49.6	38.0	28.9
H	wt.%$_{wet}$	4.3	6.43	5.2	3.2
N	wt.%$_{wet}$	0.7	0.27	1.0	0.5
S	wt.%$_{wet}$	0.8	0.43	0.3	0.1
O	wt.%$_{wet}$	21.5	24.1	19.9	23.1
Cl	wt.%$_{wet}$	0.2	0.47	0.7	0.4
H$_2$O	wt.%$_{wet}$	10.3	8.1	19.4	25.0
Ash	wt.%$_{wet}$	5.5	11.1	15.4	18.8

[a]Greco-Coppi et al. (2021); [b]Ströhle et al. (2021); [c]Haaf et al. (2020d); [d]Haaf et al. (2020a); [e]Typical limit for waste incinerators according to Velis et al. (2010)

Where $F_{CO_2}^{calc}$ and $F_{CO_2}^{carb}$ are the molar flow rates of the captured CO_2 leaving the calciner and the CO_2 leaving the carbonator, respectively. In this work, E was set as an input, and the required E_{carb} to achieve this efficiency was calculated.

The heat and product ratios are calculated with Eq. (8), where $\dot{m}_{CaO,prod}$ is the total lime production, $\dot{Q}_{in}$ is the total heat input from the fuel combustion, and the superscript ref indicates the lime production plant without carbon capture. PR is the product ratio, HR_a is the absolute heat ratio, and HR is the specific heat ratio that indicates the increase in heat input per unit of lime produced.

$$PR \equiv \frac{\dot{m}_{CaO,prod}}{\dot{m}_{CaO,prod}^{ref}}; \quad HR_a \equiv \frac{\dot{Q}_{in}}{\dot{Q}_{in}^{ref}}; \quad HR \equiv \frac{HR_a}{PR} \tag{8}$$

The KPIs introduced above are specific of the IHCaL process. Other important KPIs, which allow to compare with other carbon capture technologies, are introduced hereunder. They were selected considering relevant work in post-combustion carbon capture from cement and lime plants (De Lena et al., 2017; Ströhle et al., 2021; Voldsund et al., 2019a), especially the work within the CEMCAP project, which established a framework for comparative analysis of CO_2 capture processes for cement plants (Ananthraraman et al., 2018).

For the calculation of the specific primary energy consumption for CO_2 avoided (*SPECCA*), a procedure similar to the one considered by Haaf et al. (2020a) was adopted. The following power generation scenarios are taken into account: (i) the state-of-the-art for coal power plants (abbreviated "coal," in this work) (De Lena et al., 2018; European Union, 2015), (ii) the European energy mix (abbreviated "energy mix," in this work) calculated and used in CEMCAP (Ananthraraman et al., 2018; De Lena et al., 2018), (iii) the renewable (Ananthraraman et al., 2018), and (iii) the nuclear (Ananthraraman et al., 2018). For each of them, a reference electrical efficiency ($\eta_{ref,el}$) and a reference CO_2 emissions factor for power production ($e_{ref,el}$) are defined (see Table 6). For the scenarios (i) and (ii), these parameters are within the range of the values used normally in the literature[9]. The scenarios (iii) and (iv) are zero-CO_2-emission with $\eta_{ref,el} = 100\%$ and $\eta_{ref,el} = 33\%$, respectively. They were chosen to study the sensitivity of the results to $\eta_{ref,el}$.

The equivalent fuel consumption (q_{eq}) and the equivalent CO_2 emissions ($e_{CO2,eq}$) for the different cases can be calculated with Eq. (9).

$$q_{eq} = q + q_i; \quad e_{CO2,eq} = e_{CO2} + e_{CO2,i} \tag{9}$$

The direct fuel consumption (q) is the primary energy entering the system through the combustion of the fuels in the rotary kiln and the combustor. The indirect fuel consumption (q_i) is the primary energy consumption related to the net electric generation (or consumption) in the entire facility (P_{el}). It depends on the reference electrical efficiency $\eta_{ref,el}$:

$$q_i = \frac{P_{el}}{\eta_{ref,el}} \tag{10}$$

---

[9] $\eta_{ref,el} = 40\%$–60%; and $e_{ref,el} = 260$–760 kg$_{CO2}$/MWh$_{el}$; e.g. Bonalumi et al. (2016), De Lena et al. (2018), Martínez et al. (2018), Spinelli et al. (2018).

Table 6 Main results and KPIs for the different fuels

Parameter	Unit	Ref.	Dried lignite	RDF pellets	SRF	MSW
HR	-	1.00	3.01	3.03	3.02	3.71
HR_a	-	1.00	4.15	4.15	4.11	5.64
PR	-	1.00	1.38	1.37	1.36	1.52
E	%	-	90	90	90	90
Direct fuel consumption (*q*)	MJ_{LHV}/kg_{CaO}	5.7	17.2	17.3	17.3	21.3
Direct CO_2 emissions ($e_{CO2,d}$)	kg_{CO2}/t_{CaO}	1344	247	−378	−285	−810
State-of-the-art coal power plant ($\eta_{ref,el}$ = 44.2 %; $e_{ref,el}$ = 770 kg_{CO2}/MWh_{el})						
Indirect fuel consumption (q_i)	MJ_{LHV}/kg_{CaO}	0.25	−7.77	−7.71	−7.77	−10.52
Equivalent fuel consumption (q_{eq})	MJ_{LHV}/kg_{CaO}	5.97	9.46	9.60	9.51	10.73
Indirect CO_2 emissions ($e_{CO2,i}$)	kg_{CO2}/t_{CaO}	24	−735	−729	−734	−995
Equivalent CO_2 emissions ($e_{CO2,eq}$)	kg_{CO2}/t_{CaO}	1368	−488	−1107	−1019	−1805
SPECCA	$MJ_{LHV}/kg_{CO2,av}$	-	1.88	1.46	1.48	1.50
Energy mix (2015) EU-28 non-CHP ($\eta_{ref,el}$ = 45.9 %; $e_{ref,el}$ = 262 kg_{CO2}/MWh_{el})						
Indirect fuel consumption (q_i)	MJ_{LHV}/kg_{CaO}	0.24	−7.49	−7.43	−7.48	−10.13
Equivalent fuel consumption (q_{eq})	MJ_{LHV}/kg_{CaO}	5.97	9.75	9.88	9.80	11.12
Indirect CO_2 emissions ($e_{CO2,i}$)	kg_{CO2}/t_{CaO}	8	−250	−248	−250	−339
Equivalent CO_2 emissions ($e_{CO2,eq}$)	kg_{CO2}/t_{CaO}	1352	−3	−626	−535	−1148
SPECCA	$MJ_{LHV}/kg_{CO2,av}$	-	2.79	1.98	2.03	2.06
Renewables ($\eta_{ref,el}$ = 100 %; $e_{ref,el}$ = 0 kg_{CO2}/MWh_{el})						
Indirect fuel consumption (q_i)	MJ_{LHV}/kg_{CaO}	0.11	−3.44	−3.41	−3.43	−4.65
Equivalent fuel consumption (q_{eq})	MJ_{LHV}/kg_{CaO}	5.83	13.80	13.90	13.85	16.61
Indirect CO_2 emissions ($e_{CO2,i}$)	kg_{CO2}/t_{CaO}	0	0	0	0	0
Equivalent CO_2 emissions ($e_{CO2,eq}$)	kg_{CO2}/t_{CaO}	1344	247	−378	−285	−810
SPECCA	$MJ_{LHV}/kg_{CO2,av}$	-	7.26	4.69	4.92	5.00
Nuclear ($\eta_{ref,el}$ = 33%; $e_{ref,el}$ = 0 kg_{CO2}/MWh_{el})						
Indirect fuel consumption (q_i)	MJ_{LHV}/kg_{CaO}	0.34	−10.41	−10.33	−10.40	−14.10
Equivalent fuel consumption (q_{eq})	MJ_{LHV}/kg_{CaO}	6.06	6.83	6.98	6.88	7.16
Indirect CO_2 emissions ($e_{CO2,i}$)	kg_{CO2}/t_{CaO}	0	0	0	0	0
Equivalent CO_2 emissions ($e_{CO2,eq}$)	kg_{CO2}/t_{CaO}	1344	247	−378	−285	−810
SPECCA	$MJ_{LHV}/kg_{CO2,av}$	-	0.70	0.53	0.50	0.51

The direct CO_2 emission (e_{CO2}) is the sum of fossil CO_2 directly emitted at the stack of the facility per unit of produced lime. The CO_2 from the calcination, i.e., process emission, is considered fossil emission. For the retrofitted case with carbon capture (CC), e_{CO2} can be calculated with Eq. (11), where $\dot{m}_{CO2,foss}$ (kg_{CO2}/h) is the total fossil CO_2 emissions generation, $\dot{m}_{CO2,capt}$ (kg_{CO2}/h) is the captured CO_2, and $\dot{m}_{CaO}$ (kg_{CaO}/h) is the total production from the retrofitted plant, including the product from the IHCaL unit.

$$e_{CO2,CC} = \frac{\dot{m}_{CO2,foss} - \dot{m}_{CO2,capt}}{\dot{m}_{CaO}} \tag{11}$$

The indirect CO_2 emissions ($e_{CO2,i}$) are those associated to P_{el}. They can be calculated with Eq. (12), considering the reference CO_2 emissions factor for power production ($e_{ref,el}$) of the corresponding reference energy scenario (see Table 6).

$$e_{CO2,i} = P_{el} \cdot e_{ref,el} \tag{12}$$

The final equation for the calculation of the *SPECCA* is:

$$SPECCA = \frac{q_{eq} - q_{eq,ref}}{e_{CO2,ref} - e_{CO2}} \tag{13}$$

3 Results and discussion

In this section, the results for the analyzed cases are presented. Firstly, the specific CO_2 formation in each component is discussed. Afterwards, the results of the main KPIs are explained. Finally, the IHCaL process is compared with other post-combustion carbon capture processes.

Figure 2 shows the specific CO_2 formation in each component of the new integrated concepts (b–e), as well as the reference pilot plant without capture (a). The gray and green bars represent the fossil and biogenic specific CO_2, respectively. Direct negative CO_2 emissions are achieved for the scenarios that utilize waste-derived fuels in the combustor (Fig. 2c–e). In these cases, the total direct negative CO_2 emissions are depicted in the figure with a pink rhombus. For the reference facility and the carbon capture scenario with dried lignite (Fig. 2a–b), the direct CO_2 emissions balance is positive. The net direct CO_2 emissions are displayed with a white rhombus. No net negative direct emissions are achieved with dried lignite, since no biogenic emissions are captured.

The total specific CO_2 formation increases with the addition of the IHCaL facility (Fig. 2b–e), compared to the reference case (Fig. 2a). This is because of the CO_2 generation associated with the additional energy requirement for the carbon capture. The additional formation correlates with the fuel CO_2 emissions index ($e_{CO2,fuel}$). For fuels with lower $e_{CO2,fuel}$, the total formation is also lower, as less amount of CO_2 is generated in the combustor to supply the heat to the calciner. For this reason, the scenario with SRF has the less total formation of all the carbon capture scenarios.

If dried lignite is burnt in the combustor (Fig. 2b), the specific direct fossil CO_2 generation is almost two times that from the reference case (Fig. 2a). This means that, for dried lignite, the direct fossil CO_2 generation associated with the carbon capture is approximately
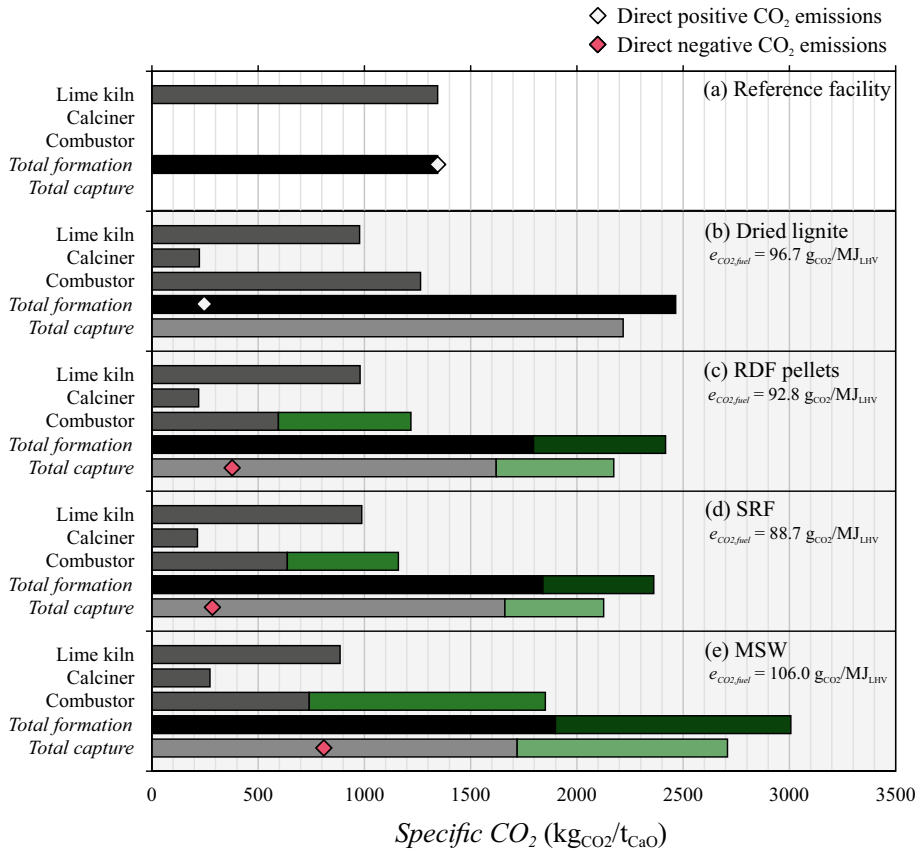
Fig. 2 Specific CO_2 formation and capture by component for all five cases considered within this study: (**a**) reference facility; and IHCaL fueled with (**b**) dried lignite, (**c**) RDF pellets, (**d**) SRF, and (**e**) MSW. The biogenic CO_2 formation is indicated with green, whereas gray represents the fossil formation. For the cases (**a**) and (**b**), the direct CO_2 balance is positive, and the total direct CO_2 emissions are displayed with a white rhombus ($\diamondsuit$). For the remaining cases, direct negative CO_2 emissions are achieved. They are indicated with a pink rhombus ($\diamondsuit$)

equal to the avoided CO_2. On the other hand, for the waste-derived fuels (Fig. 2c–e), the avoidance can be achieved without forming huge amounts of additional direct fossil CO_2 emissions (around 35% increase). The case with the lowest direct fossil CO_2 formation is the one of the RDF pellets (Fig. 2c), due to the combination of high x_{bio} with low $e_{CO2,fuel}$.

The highest variation of the formation with fuel type occurs in the combustor, where the fuel is burnt. The combustor is the most critical component regarding the direct formation of CO_2 in the IHCaL. Here, the formation is minimized by fuels with lower $e_{CO2,fuel}$. When dried lignite is used (Fig. 2b), the direct CO_2 formation in the IHCaL combustor is higher than the formation in the lime kiln. On the contrary, when RDF or SRF are utilized (Fig. 2c–d), the direct fossil generation in the combustor is much lower (61–65%). In the case of the MSW (Fig. 2e), the fossil emission of the combustor and the lime kiln are similar (84%).

The reduction of the specific CO_2 formation in the lime kiln with respect to the reference case is explained by the increase of the production, i.e., $PR > 1$. This reduction is

stronger in the scenario with MSW (Fig. 2e), because of the higher *PR*. Nevertheless, due to the high $e_{CO2,fuel}$, more CO_2 is formed from the combustion in the IHCaL; thus, this case presents the highest total direct CO_2 formation.

Due to the high biogenic fractions of the waste-derived fuels, net negative direct CO_2 emissions can be achieved in all three cases (Fig. 2c–e). The total net direct CO_2 emissions can be read from the graph as the difference between the total capture and the total fossil formation. It is indicated with a pink rhombus. The values displayed in Fig. 2 correspond only to the direct emissions, whereas the equivalent emissions are illustrated in Fig. 4.

The main results and the KPIs of the simulated scenarios are reported in Table 6. The increase in specific heat requirement due to the carbon capture (see *HR*) ranges from 201 to 271%, with respect to the reference case. The difference results from the strong influence of the $e_{CO2,fuel}$ in the heat consumption, illustrated in Fig. 3. This result is also highly dependent on Λ, as demonstrated by Greco-Coppi et al. (2021), who presented scenarios with less than 100% specific heat requirement increase for the CO_2 capture. The CO_2 formation in the combustor increases with $e_{CO2,fuel}$; thus, increasing the total captured CO_2. Due to the more demanding capture requirement, more heat is needed in the calciner and *HR* becomes higher. The direct fuel consumption, q, and the direct CO_2 emissions, $e_{CO2,d}$, increase with *HR*.

Due to the addition of the IHCaL facility, the total production increases (*PR* > 1). The increase is almost the same for lignite, RDF, and SRF and ranges from 36 to 38%. For the MSW, the production increases more (52%) because of the additional make-up requirements associated with higher CO_2 mass flows (see Fig. 2e). The product ratio can be increased by increasing the make-up rate (i.e., higher Λ). This has the effect of augmenting the production exponentially while reducing *HR* (Greco-Coppi et al., 2021).

Figure 3 illustrates the relation between HR_a and the specific CO_2 emissions for each fuel considered in this study. The HR_a rises with increasing CO_2 emissions index ($e_{CO2,fuel}$). This is due to the additional CO_2 that has to be captured from the carbonator. Other parameters such as *LHV* and the amount of hydrogen in the fuels also play a role in the variation of the heat requirements. Higher *LHV* and lower $e_{CO2,fuel}$ minimize HR_a. The range of variation represented by the gray area was calculated with the energy balance of the calciner and the combustor (see Appendix 3).
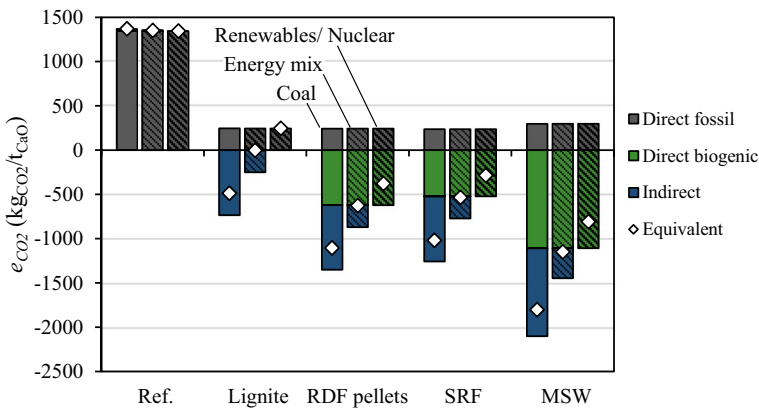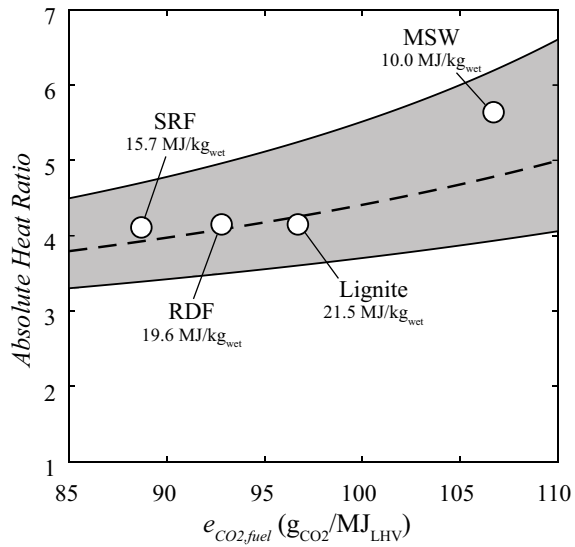
The breakdown of specific CO_2 emissions per tonne of burnt lime (product) is displayed in Fig. 4. The emissions are separated in three categories: (i) direct fossil emissions, (ii) direct biogenic emissions, and (iii) indirect emissions. The sum of all three gives the equivalent CO_2 emissions ($e_{CO2,eq}$). The results are presented for all the calculated cases, and all the considered energy scenarios. The indirect and equivalent CO_2 emissions depend on the reference efficiency of the energy scenario ($e_{ref,el}$). The results are identical for the renewable and the nuclear energy scenarios because they both have $e_{ref,el} = 0$.

The reference case, without carbon capture, presents the highest emissions level, $e_{CO2,eq}$, of 1344–1368 kg$_{CO2/tCaO}$. The major contribution comes from the direct fossil emissions corresponding to the calcination and combustion in the lime kiln. The indirect emissions are almost negligible. The results are similar for all the energy scenarios.

For the carbon capture scenarios, net negative equivalent CO_2 emissions can be achieved in every case, except when fueling lignite, for the renewables and nuclear energy scenarios. If waste-derived fuels are used, the highest contribution to the negative emissions corresponds to the captured biogenic CO_2, which is independent from the energy scenario. The indirect emissions are strongly dependent on $e_{ref,el}$ because of the relatively high power generation in the retrofitted plants (42–63 MW$_{el}$). With waste-derived fuels, negative emissions as high as -1805 kgCO$_2$/t$_{CaO}$ can be achieved. This corresponds to an equivalent CO_2 avoidance of over 230%.

The *SPECCA* is one of the most important thermodynamic KPIs. It represents the primary energy consumption associated with the CO_2 avoidance. In Fig. 5, the

Fig. 3 Absolute heat ratio and CO_2 specific emissions for the fuels considered in this work. The circles represent the results of the simulations corresponding to each of the fuels. The gray area represents the theoretical increase of the heat requirement with the CO_2-specific emission, for a wide range of fuels


Fig. 4 Specific CO_2 emissions for the different fuels considered within this work. The breakdown of the emissions is depicted with bars. The power generation scenarios are indicted with the filling type (solid, hatched). The equivalent specific CO_2 emissions ($e_{CO2,eq}$) are displayed with a rhombus (◇)

breakdown of *SPECCA* for all the carbon capture scenarios is displayed, considering (i) the CO_2 compression power requirement, (ii) the power requirement increase (without compression), (iii) the fuel requirement increase, and (iv) the power generation. The values are presented for the energy scenarios utilized throughout this work. Because of the high power generation (light blue bar in Fig. 5), the results depend strongly on the reference power generation efficiency ($\eta_{ref,el}$). The lower the $\eta_{ref,el}$, the better the results in terms of SPECCA. The values corresponding to the European energy mix scenario are higher than for the state-of-the-art coal power plant due to the lower associated CO_2 avoided (see Fig. 4). In the same way, the *SPECCA* values
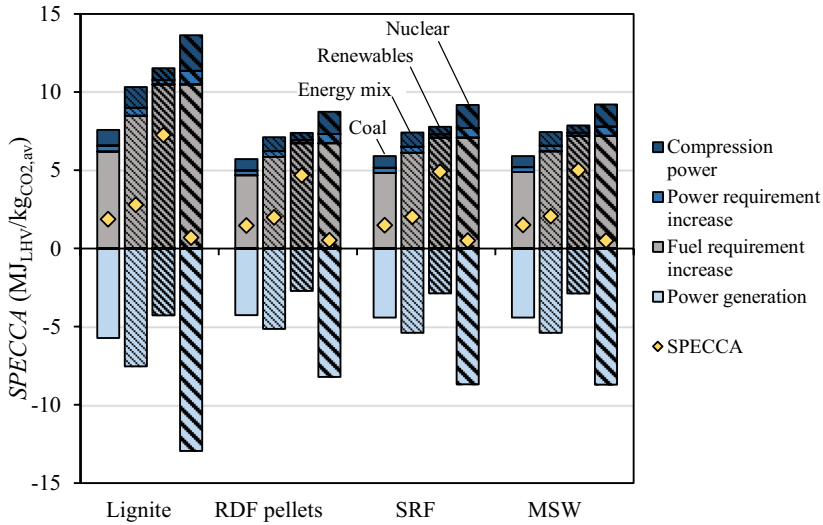
Fig. 5 *SPECCA* breakdown for all the carbon capture scenarios analyzed in this work. Each category of the breakdown is indicated with solid bars (state-of-the-art coal power plant) and hatched bars (energy mix, renewables, and nuclear). The *SPECCA* values are displayed with a rhombus ($\diamondsuit$)

of the lignite scenario are relatively high because of the low CO_2 avoidance compared to the waste-derived fuels that allow for net negative CO_2 emissions. When compared with an oxy-fired CaL process, the *SPECCA* values presented in this work are in general much lower, mainly because of the avoided penalty of the ASU, which increases the total *SPECCA* by approximately 1 $MJ_{LHV}/kg_{CO2,av}$ in the European mix scenario (De Lena et al., 2022). Nevertheless, for the renewable scenario, relatively high values were obtained because of the high $\eta_{ref,el}$. These values are discussed hereunder.
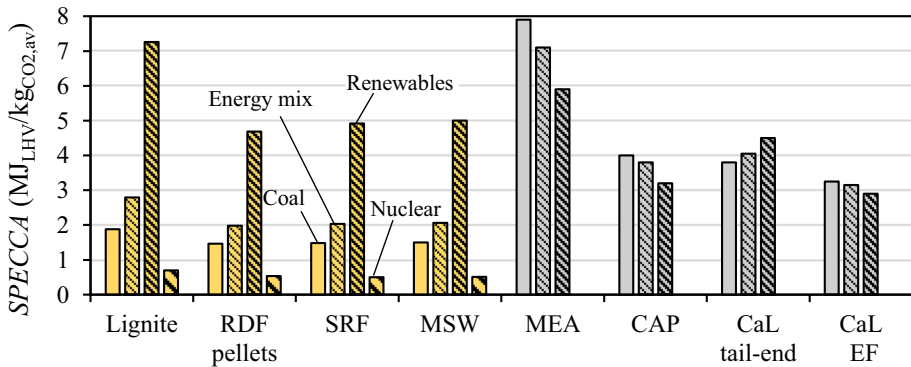
Fig. 6 *SPECCA* comparison between the different fuels considered within this work and other post-combustion carbon capture processes: monoethanolamine absorption (MEA), chilled ammonia process (CAP), tail-end directly heated carbonate looping (CaL), and entrained flow (EF) directly heated CaL. The reference data for MEA, CAP, CaL tail-end, and CaL EF was obtained from Voldsund et al. (2019a), who considered the application of these technologies in the cement production process. No data was available for the nuclear scenario

In Fig. 6, the *SPECCA* values of different post-combustion carbon capture processes are compared with the ones corresponding to the IHCaL scenarios, for the different energy scenarios considered in this work. The selected post-combustion CO_2 capture processes for this comparison are: (i) monoethanolamine absorption (MEA), a technologically ready process; (ii) chilled ammonia process (CAP); (iii) tail-end directly heated CaL; and (iv) entrained flow (EF) directly heated CaL. As a reference for the MEA, CAP, and CaL technologies, the *SPECCA* data from the CEMCAP project was used (Voldsund et al., 2019a). These values were calculated for cement production, which is similar to lime production, as discussed in the introductory chapter. It can be seen that the *SPECCA* of the IHCaL scenarios is considerably lower than the ones reported for the other carbon capture methods, except for the renewable scenarios. The IHCaL process allows for CO_2 capture with very low primary energy consumption, less than 2.1 $MJ_{LHV}/kg_{CO2,av}$, when using waste-derived fuel. Nevertheless, the *SPECCA* values increase drastically for the renewable scenario. Thereby, the electrical power is considered equivalent as the primary energy; thus, the additional power generation in the IHCaL process is not advantageous as in the other scenarios. Furthermore, the assumption of $\eta_{ref,el} = 100\%$ associated with this scenario is unfairly high considering the type of feedstock involved.

The main challenge of the IHCaL process is the significant increase in the absolute heat required for the capture, i.e., HR_a, which is around 30% higher than for an oxy-fired CaL process[10]. Nonetheless, dynamic investment models suggest that the IHCaL technology would be superior in terms of global economic performance, compared to other post-combustion CO_2 capture processes (Junk et al., 2016). Within the ANICA Project, the concepts presented in this work are being evaluated to assess their viability in terms of CO_2 avoidance costs and environmental impact (Ströhle et al., 2021).

4 Conclusion

An innovative CO_2 post-combustion carbon capture method, the IHCaL process, was analyzed in this work. The configuration presented is suitable for retrofitting lime and cement plants. To evaluate its performance with alternative fuel firing, mass and heat balances with different fuels were performed, and the most relevant KPIs were calculated.

From the direct emissions breakdown, it was shown that the combustor influences the direct formation of CO_2 the most. The direct CO_2 formation is minimized by fuels with a lower CO_2 emissions index, $e_{CO2,fuel}$. Additionally, the utilization of dried lignite yielded an increase of approximately 100% in the total direct fossil CO_2 formation. This means that the additional generation associated with the carbon capture was approximately equal to the avoided CO_2. With this consideration, it appears more reasonable to use waste-derived fuels for the tail-end IHCaL, whereby the increase in total direct fossil CO_2 formation linked to the avoidance is relatively low (around 30%).

The results show that very low *SPECCA* values can be achieved for three of the simulated scenarios[11]: from 0.50 to 2.79 $MJ_{LHV}/kg_{CO2,av}$. In particular, *SPECCA* values between 0.50 and 1.98 $MJ_{LHV}/kg_{CO2,av}$ were achieved for the scenarios utilizing waste-derived fuels in the combustor. By reason of its low primary energy requirements[12], the IHCaL process is a very promising

---

[10] Estimated by comparing the results from this work with the total heat input increase reported by De Lena et al. (2017) in the analysis of an integrated CaL-process for CO_2 capture in cement plants.

[11] State-of-the-art coal power plant, energy mix (2015), and nuclear.

[12] When comparing these *SPECCA* values with the available literature for other post-combustion carbon capture processes for lime and cement plants: De Lena et al. (2022), De Lena et al. (2019), De Lena et al. (2017), Voldsund et al. (2019a), Voldsund et al. (2019b).

retrofitting technology for carbon capture from lime and cement plants. It may be deployed in scenarios, in which the associated power generation is an advantage. This is not the case for the 100% renewables scenario, which assumes the same worth for generated power and primary energy ($\eta_{ref,el} = 100\%$). For this scenario, the *SPECCA* values were higher than 4.6 MJ_{LHV}/$kg_{CO2,av}$.

Furthermore, it was demonstrated that the IHCaL process is suitable for achieving net negative CO_2 emissions; thus, carbon dioxide removal (CDR). For all the scenarios, the highest negative emissions were obtained with MSW fuel. Net negative emissions as high as -1805 kg_{CO2}/t_{CaO} were achieved[13]. This value represents an equivalent CO_2 avoidance of more than 230%, with respect to the reference plant without capture (1368 kg_{CO2}/t_{CaO}).

The IHCaL process is particularly suitable for fuels with a high biogenic fraction (x_{bio}) and low specific CO_2 emissions ($e_{CO2,fuel}$). This combination of properties can be found in high caloric SRF, such as the one considered in this work (class 3 SRF, according to DIN EN ISO, 2021). The utilization of these fuels in the IHCaL combustor allows for net negative CO_2 emissions (-1019 kg_{CO2}/t_{CaO}) with very low *SPECCA* (1.48 MJ_{LHV}/$kg_{CO2,av}$)[14].

Appendix 1. Additional input data

The fuel data used for the calculations in this work are provided in Table 7.

The carbonator was modeled based on the work of Lasheras et al. (2011). The main model assumptions are reported in Table 8. The governing equations for the carbonation model were:

$$\frac{1}{K_r} = \frac{d_p}{6 \cdot K_g} + \frac{1}{K_{ri}}$$
$$K_g = \frac{D_{CO2}}{d_p \cdot Sh}$$
$$K_{ri} = k_s \cdot \frac{X_{b,N} \cdot S_0 \cdot \rho_{CaO}}{M_{CaO}} \cdot (1 - X)^{2/3}$$

(14)

K_r is the global reaction rate, K_g and K_{ri} are the diffusion-controlled rate and the chemical rate, respectively, d_p is the particle diameter, and *Sh* is the Sherwood dimensionless number. *X* is the conversion, i.e., fraction of active sorbent that has been carbonated. The rest of the constants are defined in Table 8. The active fraction of CaO ($X_{b,N}$) was calculated with the deactivation model of Abanades et al. (2005), according to Eq. (15).

$$X_{b,N} = \frac{f_m \cdot (1 - f_w) \cdot F_0}{F_0 + F_R \cdot (1 - f_m)} + f_w$$

(15)

---

[13] Utilizing MSW in the combustor; calculated with the state-of-the-art coal power plant energy scenario ($\eta_e = 44.2\%$; $e_{ref,el} = 770$ kg_{CO2}/MWh_{el}).

[14] Calculated with the state-of-the-art coal power plant energy scenario ($\eta_e = 44.2\%$; $e_{ref,el} = 770$ kg_{CO2}/MWh_{el}).

Table 7 Detailed fuel data used in this work

Property	Dried lignite	RDF pellets	SRF	MSW
Proximate analysis (%$_{dry}$)				
Moisture content	10.3	8.1	19.4	25.0
Fix carbon	63.2	54.0	47.2	38.5
Volatile matter	30.7	33.9	33.7	36.4
Ash content	6.1	12.1	19.1	25.1
Ultimate analysis (%$_{dry}$)				
Carbon	63.2	54.0	47.2	38.5
Hydrogen	4.8	7.0	6.5	4.3
Nitrogen	0.8	0.3	1.2	0.7
Chlorine	0.2	0.5	0.9	0.5
Sulfur	0.9	0.5	0.4	0.1
Oxygen	24.0	25.7	24.7	30.8
Ash	6.1	12.1	19.1	25.1
Higher heating value (HHV_{dry}) (MJ/kg$_{dry}$)	25.3	23.1	21.5	15.1
Lower heating value (LHV_{wet}) (MJ/kg$_{wet}$)	21.5	19.6	15.7	10.0

Table 8 Inputs for the carbonator reactor model

Parameter	Symbol	Unit	Value
Main inputs			
Make-up rate	Λ	mol$_{CaCO3}$/mol$_{CO2}$	0.10
Carbonator operating temperature	T_{carb}	°C	650
Free-gas velocity	u_0	m/s	4.5
Carbonator total height	h_{total}	m	15
Carbonator pressure drop	Δp_{carb}	mbar	100
Inputs for hydrodynamic model			
Mean particle diameter	$d_{p,50}$	µm	180
Decay constant lean region	a	-	3
Volume fraction at dense region	ε_{sd}	-	0.16
Inputs for carbonation reaction model			
Effective gas diffusivity of CO_2 in air	D_{CO2}	m^2/s	$8.75 \cdot 10^{-5}$
Initial specific surface area	S_0	m^2/m^3	$1.70 \cdot 10^7$
Carbonation rate constant	k_s	m^4/(s·mol)	$5.95 \cdot 10^{-10}$

Appendix 2. Detailed results

See Tables 9, 10, 11, 12, and 13.

Table 9 Results from the power calculations in MW_e

	Ref.	Dried lignite	RDF pellets	SRF	MSW
$P_{compression}$	0.0	7.6	7.4	7.2	10.2
$P_{blowers}$	0.0	3.2	3.4	3.3	4.6
P_{kiln}	0.7	0.7	0.7	0.7	0.7
$P_{in,total}$	0.7	11.5	11.5	11.2	15.6
$P_{out,total}$	0.0	43.1	42.8	42.4	62.7

Table 10 CO_2 formation in kg_{CO_2}/t_{CaO}, detailed results

	Component	Fossil	Biogenic	Total
Reference facility	Lime kiln	1344	0	1344
	Calciner	0	0	0
	Combustor	0	0	0
	Total formation	*1344*	*0*	*1344*
	Total capture	*0*	*0*	*0*
Dried lignite	Lime kiln	977	0	977
	Calciner	224	0	224
	Combustor	1264	0	1264
	Total formation	*2465*	*0*	*2465*
	Total capture	*2218*	*0*	*2218*
RDF pellets	Lime kiln	980	0	980
	Calciner	220	0	220
	Combustor	596	623	1219
	Total formation	*1796*	*622*	*2418*
	Total capture	*1620*	*554*	*2174*
SRF	Lime kiln	988	0	988
	Calciner	215	0	215
	Combustor	638	522	1160
	Total formation	*1841*	*522*	*2362*
	Total capture	*1661*	*464*	*2126*
MSW	Lime kiln	885	0	885
	Calciner	274	0	274
	Combustor	741	1111	1852
	Total formation	*1900*	*1108*	*3007*
	Total capture	*1719*	*990*	*2709*

Table 11 Result from CO_2 emission calculations in kg_{CO2}/t_{CaO} considering different energy scenarios

	Ref.	Dried lignite	RDF pellets	SRF	MSW
Direct CO_2 emissions					
Fossil	1344	245	244	237	298
Biogenic	0	0	−622	−522	−1108
Total	*1344*	*245*	*−378*	*−285*	*−810*
Indirect CO_2 emissions					
Coal	24	−735	−729	−734	−995
Energy mix	8	−250	−248	−250	−339
Renewables	0	0	0	0	0
Nuclear	0	0	0	0	0
Equivalent CO_2 emissions					
Coal	1368	−488	−1107	−1019	−1805
Energy mix	1352	−3	−626	−535	−1148
Renewables	1344	247	−378	−285	−810
Nuclear	1344	247	−378	−285	−810

Table 12 Results of *SPECCA* breakdown in $MJ_{LHV}/kg_{CO2,av}$

Energy scenario	*SPECCA* breakdown	Dried lignite	RDF pellets	SRF	MSW
Coal	Fuel requirement increase	6.20	4.68	4.84	4.90
	Power requirement increase	0.38	0.31	0.31	0.30
	CPU power requirement	1.01	0.74	0.75	0.72
	Power generation	−5.71	−4.27	−4.42	−4.41
	Total	*1.88*	*1.46*	*1.48*	*1.50*
Energy mix	Fuel requirement increase	8.49	5.86	6.12	6.21
	Power requirement increase	0.51	0.37	0.38	0.36
	CPU power requirement	1.33	0.89	0.91	0.88
	Power generation	−7.53	−5.14	−5.39	−5.39
	Total	*2.79*	*1.98*	*2.03*	*2.06*
Renewables	Fuel requirement increase	10.49	6.73	7.09	7.21
	Power requirement increase	0.29	0.20	0.20	0.19
	CPU power requirement	0.75	0.47	0.49	0.47
	Power generation	−4.27	−2.71	−2.86	−2.87
	Total	*7.26*	*4.69*	*4.92*	*5.00*
Nuclear	Fuel requirement increase	10.49	6.73	7.09	7.21
	Power requirement increase	0.87	0.59	0.62	0.58
	CPU power requirement	2.28	1.42	1.47	1.42
	Power generation	−12.94	−8.21	−8.68	−8.70
	Total	*0.70*	*0.53*	*0.50*	*0.51*

Table 13 Results for the carbonator reactor model: variables from the process model and reactor model results

Parameter	Unit	Dried lignite	RDF pellets	SRF	MSW
Inputs from process model					
$y_{CO2,in}$	mol/mol	0.16	0.15	0.15	0.15
$T_{FlueGas}$	°C	269	269	269	269
F_{CO2}	mol/s	468	458	444	630
Results from reactor model					
Φ	mol_{Ca}/mol_{CO2}	5.40	5.50	5.60	5.65
X_{bN}	mol_{CaCO3}/mol_{Ca}	0.190	0.190	0.189	0.189
X_{carb}	mol_{CaCO3}/mol_{Ca}	0.167	0.161	0.161	0.161
E_{carb}	%	89	89	89	89
τ_{carb}	min	5.3	5.6	5.7	5.5
h_{bed}	m	3.3	3.3	3.3	3.3
Specific inventory	kg/m^2	1020	1020	1020	1020

Appendix 3. Calculation of heat ratio for different fuels

For the calculation of the heat requirement in the combustor, for any fuel, the heat balance of the system calciner-combustor is performed.

$$\{combustion\ heat\} = \{heat\ requirement\ calciner\} + \{sensible\ heat\ loss\ in\ combustor\}$$

$$\dot{Q}_{comb} = \dot{m}_{fuel} \cdot LHV_{wet} = F_{CO2} \cdot \Psi_1 + \dot{m}_{fuel} \cdot \Psi_2$$

(16)

This equation can be solved using the specific heat capacities of the substances (c_p) and the operational parameters of the IHCaL facility:

$$\Psi_1 = \left(\Lambda + \Phi \cdot X_{carb}\right) \cdot E_{calc} \cdot \Delta H_{calc} + \left(T_{calc} - T_{sorb,calc,in}\right) \cdot \left[\left(\Lambda + \Phi \cdot X_{carb}\right) \cdot \bar{c}_{p,CaCO3} + \left(1 - X_{carb}\right) \cdot \bar{c}_{p,CaO}\right]$$
$$\Psi_2 = AFR \cdot c_{p,air} \cdot \left(T_{comb} - T_{preheat}\right) + c_{p,fuel} \cdot \left(T_{comb} - T_0\right)$$
$$\dot{Q}_{comb} = F_{CO2,plant} \cdot \Psi_1 \cdot \left(1 - \frac{e_{CO2,fuel}}{M_{CO2}} \cdot \Psi_1 + \frac{\Psi_2}{LHV}\right)^{-1}$$

(17)

The values assumed for the calculation of the curves of Fig. 3 are reported in Table 14.

Table 14 Values for the calculation of typical heat ratios for different $e_{CO2,fuel}$

Parameter	Unit	Bottom boundary	Base value	Top boundary
$\dot{F}_{CO2,plant}$	kmol/h		735	
$\dot{Q}_{ref}$	MW$_{th}$		38.7	
E_{calc}	%		99	
E_{carb}	%		88	
Λ	mol$_{CaCO3}$/mol$_{CO2}$		0.1	
T_{calc}	°C		900	
$T_{sorb,calc,in}$	°C		810	
$T_{preheat}$	°C		800	
T_{comb}	°C		1000	
T_0	°C		20	
$c_{p,air}$	kJ/(kg·K)		1.1	
$\overline{c}_{p,CaO}$	J/(mol·K)		51.7	
$\overline{c}_{p,CaCO3}$	J/(mol·K)		131.3	
Φ	mol$_{Ca}$/mol$_{CO2}$	5.2	5.5	5.8
LHV_{wet}	MJ/kg$_{wet}$	22.0	15.5	9.0
Air-fuel ratio (AFR) [a]	kg$_{air}$/kg$_{fuel}$	9.0	9.0	4.8
$c_{p,fuel}$ [b]	kJ/(kg·K)	1.0	1.25	1.50

[a]Lignite (base and bottom) and RDF (top). Data from Liu et al. (2020), with $\lambda = 1.2$

[b]Based on data from Savage (1989) and Strezov et al. (2004)

Data availability The datasets generated and analyzed during the current study are available from the corresponding author on reasonable request.

Declarations

Competing interests The authors Martin Greco-Coppi, Carina Hofmann, Jochen Ströhle, Bernd Epple, and Diethelm Walter filed a patent application titled "Apparatus and Method for Producing Lime", Assignees: Technical University of Darmstadt and Lhoist Germany Rheinkalk GmbH, patent pending before the German Patent and Trademark Office, Application number 10 2023 114 354.9.

References

Abanades JC, Anthony EJ, Lu DY, Salvador C, Alvarez D (2004) Capture of CO_2 from combustion gases in a fluidized bed of CaO. AICHE J 50:1614–1622. https://doi.org/10.1002/aic.10132

Abanades JC, Anthony EJ, Wang J, Oakey JE (2005) Fluidized bed combustion systems integrating CO_2 capture with CaO. Environ Sci Technol 39:2861–2866. https://doi.org/10.1021/es0496221

Anantharaman R, Berstad D, Cinti G, Gatti M (2018) D3.2 CEMCAP framework for comparative techno-economic analysis of CO_2 capture from cement plants

Arias B, Alonso M, Abanades C (2017a) CO_2 capture by calcium looping at relevant conditions for cement plants: experimental testing in a 30 kW_{th} pilot plant. Ind Eng Chem Res 56:2634–2640. https://doi.org/10.1021/acs.iecr.6b04617

Arias B, Diego ME, Abanades JC, Lorenzo M, Diaz L, Martínez D, Alvarez J, Sánchez-Biezma A (2013) Demonstration of steady state CO_2 capture in a 1.7MW_{th} calcium looping pilot. Int J Greenh Gas Control 18:237–245. https://doi.org/10.1016/j.ijggc.2013.07.014

Arias B, Diego ME, Méndez A, Abanades JC, Díaz L, Lorenzo M, Sanchez-Biezma A (2017b) Operating experience in la Pereda 1.7 MW_{th} calcium looping pilot. Energy Procedia 114:149–157. https://doi.org/10.1016/j.egypro.2017.03.1157

Astolfi M, De Lena E, Romano MC (2019) Improved flexibility and economics of calcium looping power plants by thermochemical energy storage. Int J Greenh Gas Control 83:140–155. https://doi.org/10.1016/j.ijggc.2019.01.023

Astrup T, Møller J, Fruergaard T (2009) Incineration and co-combustion of waste: accounting of greenhouse gases and global warming contributions. Waste Manag Res 27:789–799. https://doi.org/10.1177/0734242X09343774

Barker DJ, Turner SA, Napier-Moore PA, Clark M, Davison JE (2009) CO_2 capture in the cement industry. Energy Procedia 1:87–94. https://doi.org/10.1016/j.egypro.2009.01.014

Bhatt M, Chakinala AG, Joshi JB, Sharma A, Pant KK, Shah K, Sharma A (2021) Valorization of solid waste using advanced thermo-chemical process: a review. J Environ Chem Eng 9:105434. https://doi.org/10.1016/j.jece.2021.105434

Bonalumi D, Valenti G, Lillia S, Fosbøl PL, Thomsen K (2016) A layout for the carbon capture with aqueous ammonia without salt precipitation. Energy Procedia 86:134–143. https://doi.org/10.1016/j.egypro.2016.01.014

Busch P, Kendall A, Murphy CW, Miller SA (2022) Literature review on policies to mitigate GHG emissions for cement and concrete. Resour Conserv Recycl 182:106278. https://doi.org/10.1016/j.resconrec.2022.106278

Carbone C, Ferrario D, Lanzini A, Stendardo S, Agostini A (2022) Evaluating the carbon footprint of cement plants integrated with the calcium looping CO_2 capture process. Front Sustain 3:809231. https://doi.org/10.3389/frsus.2022.809231

Carrasco F, Grathwohl S, Maier J, Ruppert J, Scheffknecht G (2019) Experimental investigations of oxyfuel burner for cement production application. Fuel 236:608–614. https://doi.org/10.1016/j.fuel.2018.08.135

Carrasco-Maldonado F, Spörl R, Fleiger K, Hoenig V, Maier J, Scheffknecht G (2016) Oxy-fuel combustion technology for cement production – state of the art research and technology development. Int J Greenh Gas Control 45:189–199. https://doi.org/10.1016/j.ijggc.2015.12.014

Charitos A, Rodríguez N, Hawthorne C, Alonso M, Zieba M, Arias B, Kopanakis G, Scheffknecht G, Abanades JC (2011) Experimental validation of the calcium looping CO_2 capture process with two circulating fluidized bed carbonator reactors. Ind Eng Chem Res 50:9685–9695. https://doi.org/10.1021/ie200579f

Chen X, Jin X, Ling X, Wang Y (2020) Exergy analysis of concentrated solar power plants with thermochemical energy storage based on calcium looping. ACS Sustain Chem Eng 8:7928–7941. https://doi.org/10.1021/acssuschemeng.0c01586

Clarke L, Jiang K, Akimoto K, Babiker M, Blanford G, Fisher-Vanden K, Hourcade JC, Krey V, Kriegler E, Löschel A (2014) Assessing transformation pathways. In: Change IPoC, Edenhofer O (eds) Climate change 2014: mitigation of climate change; working group III contribution to the fifth assessment report of the intergovernmental panel on climate change. Cambridge University Press, New York, pp 413–510

De Lena E, Arias B, Romano MC, Abanades JC (2022) Integrated calcium looping system with circulating fluidized bed reactors for low CO_2 emission cement plants. Int J Greenh Gas Control 114:103555. https://doi.org/10.1016/j.ijggc.2021.103555

De Lena E, Spinelli M, Gatti M, Scaccabarozzi R, Campanari S, Consonni S, Cinti G, Romano MC (2019) Techno-economic analysis of calcium looping processes for low CO_2 emission cement plants. Int J Greenh Gas Control 82:244–260. https://doi.org/10.1016/j.ijggc.2019.01.005

De Lena E, Spinelli M, Martínez I, Gatti M, Scaccabarozzi R, Cinti G, Romano MC (2017) Process integration study of tail-end Ca-looping process for CO_2 capture in cement plants. Int J Greenh Gas Control 67:71–92. https://doi.org/10.1016/j.ijggc.2017.10.005

De Lena E, Spinelli M, Romano MC (2018) CO_2 capture in cement plants by "tail-end" calcium looping process. Energy Procedia 148:186–193. https://doi.org/10.1016/j.egypro.2018.08.049

Dean C, Hills T, Florin N, Dugwell D, Fennell PS (2013) Integrating calcium looping CO_2 capture with the manufacture of cement. Energy Procedia 37:7078–7090. https://doi.org/10.1016/j.egypro.2013.06.644

Diego ME, Arias B, Abanades JC (2016a) Analysis of a double calcium loop process configuration for CO_2 capture in cement plants. J Clean Prod 117:110–121. https://doi.org/10.1016/j.jclepro.2016.01.027

Diego ME, Arias B, Abanades JC (2020) Investigation of the dynamic evolution of the CO_2 carrying capacity of solids with time in La Pereda 1.7 MW_{th} calcium looping pilot plant. Int J Greenh Gas Control 92:102856. https://doi.org/10.1016/j.ijggc.2019.102856

Diego ME, Arias B, Méndez A, Lorenzo M, Díaz L, Sánchez-Biezma A, Abanades JC (2016b) Experimental testing of a sorbent reactivation process in La Pereda 1.7 MW_{th} calcium looping pilot plant. Int J Greenh Gas Control 50:14–22. https://doi.org/10.1016/j.ijggc.2016.04.008

Dieter H, Bidwe AR, Varela-Duelli G, Charitos A, Hawthorne C, Scheffknecht G (2014) Development of the calcium looping CO_2 capture technology from lab to pilot scale at IFK, University of Stuttgart. Fuel 127:23–37. https://doi.org/10.1016/j.fuel.2014.01.063

DIN EN (2011) Solid recovered fuels - Methods for the determination of biomass content; German version EN 15440:2011

DIN EN ISO (2021) Solid recovered fuels - Specifications and classes (ISO 21640:2021); German version EN ISO 21640:2021

Epple B (2009) Method and arrangement for separation of CO_2 from combustion flue gas (U.S. Patent No. US2010/0086456A1). U.S. Patent and Trademark Office

Erans M, Hanak D, Mir J, Anthony E, Manovic V (2016) Process modelling and techno-economic analysis of natural gas combined cycle integrated with calcium looping. Therm Sci 20:59–67. https://doi.org/10.2298/TSCI151001209E

Eriksson M, Hökfors B, Backman R (2014) Oxyfuel combustion in rotary kiln lime production. Energy Sci Eng 2:204–215. https://doi.org/10.1002/ese3.40

European Union (2015) L335/54: reviewing harmonised efficiency reference values for separate production of electricity and heat in application of Directive 2012/27/EU of the European parliament and of the council and repealing commission implementing decision 2011/877/EU. Official Journal of the European Union

Fantini M, Balocco M, Buzzi L, Canonico F, Consonni S, Cremona R, Gatti M, Hammerich J, Koehler R, Magli F, Romano MC, Spinelli M (2021) Calcium looping technology demonstration in industrial environment: status of the CLEANKER pilot plant. SSRN J. https://doi.org/10.2139/ssrn.3817346

Furimsky E (2007) Carbon dioxide emission index as a mean for assessing fuel quality. Energ Sourc Part A 30:119–131. https://doi.org/10.1080/15567030600820583

Fuss S, Canadell JG, Peters GP, Tavoni M, Andrew RM, Ciais P, Jackson RB, Jones CD, Kraxner F, Nakicenovic N, Le Quéré C, Raupach MR, Sharifi A, Smith P, Yamagata Y (2014) Betting on negative emissions. Nat Clim Chang 4:850–853. https://doi.org/10.1038/nclimate2392

Fuss S, Lamb WF, Callaghan MW, Hilaire J, Creutzig F, Amann T, Beringer T, de Oliveira Garcia W, Hartmann J, Khanna T, Luderer G, Nemet GF, Rogelj J, Smith P, Vicente JLV, Wilcox J, Del Mar Zamora Dominguez M, Minx JC (2018) Negative emissions—Part 2: costs, potentials and side effects. Environ Res Lett 13:63002. https://doi.org/10.1088/1748-9326/aabf9f

Gardarsdottir S, de Lena E, Romano M, Roussanaly S, Voldsund M, Pérez-Calvo J-F, Berstad D, Fu C, Anantharaman R, Sutter D, Gazzani M, Mazzotti M, Cinti G (2019) Comparison of technologies for CO_2 capture from cement production—part 2: cost analysis. Energies 12:542. https://doi.org/10.3390/en12030542

Garðarsdóttir SÓ, Normann F, Skagestad R, Johnsson F (2018) Investment costs and CO_2 reduction potential of carbon capture from industrial plants – a Swedish case study. Int J Greenh Gas Control 76:111–124. https://doi.org/10.1016/j.ijggc.2018.06.022

Gerassimidou S, Velis CA, Williams PT, Komilis D (2020) Characterisation and composition identification of waste-derived fuels obtained from municipal solid waste using thermogravimetry: a review. Waste Manag Res 38:942–965. https://doi.org/10.1177/0734242X20941085

Grasa GS, Abanades JC (2006) CO_2 capture capacity of CaO in long series of carbonation/calcination cycles. Ind Eng Chem Res 45:8846–8851. https://doi.org/10.1021/ie0606946

Greco-Coppi M, Hofmann C, Ströhle J, Walter D, Epple B (2021) Efficient CO_2 capture from lime production by an indirectly heated carbonate looping process. Int J Greenh Gas Control 112:103430. https://doi.org/10.1016/j.ijggc.2021.103430

Grote K-H, Feldhusen J (eds) (2007) Dubbel: Taschenbuch für den Maschinenbau, 22nd edn. Springer-Verlag, Berlin, Heidelberg, New York

Haaf M, Anantharaman R, Roussanaly S, Ströhle J, Epple B (2020a) CO_2 capture from waste-to-energy plants: techno-economic assessment of novel integration concepts of calcium looping technology. Resour Conserv Recycl 162:104973. https://doi.org/10.1016/j.resconrec.2020.104973

Haaf M, Hilz J, Peters J, Unger A, Ströhle J, Epple B (2020b) Operation of a 1 MW_{th} calcium looping pilot plant firing waste-derived fuels in the calciner. Powder Technol 372:267–274. https://doi.org/10.1016/j.powtec.2020.05.074

Haaf M, Ohlemüller P, Ströhle J, Epple B (2020c) Techno-economic assessment of alternative fuels in second-generation carbon capture and storage processes. Mitig Adapt Strateg Glob Chang 25:149–164. https://doi.org/10.1007/s11027-019-09850-z

Haaf M, Peters J, Hilz J, Unger A, Ströhle J, Epple B (2020d) Combustion of solid recovered fuels within the calcium looping process – experimental demonstration at 1 MW_{th} scale. Exp Thermal Fluid Sci 113:110023. https://doi.org/10.1016/j.expthermflusci.2019.110023

Hills TP (2016) Investigations of the use of spent sorbent from the Ca looping process in cement manufacture and investigation of long-term CO_2 uptake in cement and concrete. PhD Thesis. Imperial College London of Science, Technology and Medicine.   https://doi.org/10.25560/39286

Hilz J, Helbig M, Haaf M, Daikeler A, Ströhle J, Epple B (2017) Long-term pilot testing of the carbonate looping process in 1 MW_{th} scale. Fuel 210:892–899. https://doi.org/10.1016/j.fuel.2017.08.105

Hilz J, Helbig M, Haaf M, Daikeler A, Ströhle J, Epple B (2018) Investigation of the fuel influence on the carbonate looping process in 1 MW_{th} scale. Fuel Process Technol 169:170–177. https://doi.org/10.1016/j.fuproc.2017.09.016

Hoeftberger D, Karl J (2013) Self-fluidization in an indirectly heated calciner. Chem Eng Technol 36:1533–1538. https://doi.org/10.1002/ceat.201300111

Hoeftberger D, Karl J (2016) The indirectly heated carbonate looping process for CO_2 capture—a concept with heat pipe heat exchanger. J Energy Resour Technol 138(042211):148A. https://doi.org/10.1115/1.4033302

Hofmann C, Greco-Coppi M, Ströhle J, Epple B (2022a) Operation of a 300 kW_{th} indirectly heated carbonate looping pilot plant for CO_2 capture from lime industry. Fluidized Bed Conversion Conference, 8-11 May 2022, Chalmers University of Technology (Sweden)

Hofmann C, Greco-Coppi M, Ströhle J, Epple B (2022b) Pilot testing of the indirectly heated carbonate looping process for cement and lime plants. Proceedings of the 16th Greenhouse Gas Control Technologies Conference (GHGT-16) 23-24 Oct 2022. https://doi.org/10.2139/ssrn.4278810

Hornberger M, Moreno J, Schmid M, Scheffknecht G (2020) Experimental investigation of the carbonation reactor in a tail-end calcium looping configuration for CO_2 capture from cement plants. Fuel Process Technol 210:106557. https://doi.org/10.1016/j.fuproc.2020.106557

Hornberger M, Moreno J, Schmid M, Scheffknecht G (2021) Experimental investigation of the calcination reactor in a tail-end calcium looping configuration for CO_2 capture from cement plants. Fuel 284:118927. https://doi.org/10.1016/j.fuel.2020.118927

IEA (2020a) Energy technology perspectives 2020 - special report on carbon capture utilisation and storage: CCUS in clean energy transitions. OECD; OECD Publishing, Paris

IEA (2020b) Projected Costs of Generating Electricity, Paris

IPCC (2018) Global warming of 1.5°C: an IPCC special report on the impacts of global warming of 1.5°C above pre-industrial levels and related global greenhouse gas emission pathways, in the context of strengthening the global response to the threat of climate change

IPCC (2022) Climate change 2022: mitigation of climate change. Contribution of Working Group III to the Sixth Assessment Report of the Intergovernmental Panel on Climate Change

Jackson S, Brodal E (2019) Optimization of the energy consumption of a carbon capture and sequestration related carbon dioxide compression processes. Energies 12:1603. https://doi.org/10.3390/en12091603

Jafarian M, Dally BB, Nathan GJ (2022) Hydrogen peroxide for fuel oxidation to achieve CO_2 capture from lime production. Energy Convers Manag X 15:100276. https://doi.org/10.1016/j.ecmx.2022.100276

Junk M, Reitz M, Ströhle J, Epple B (2013) Thermodynamic evaluation and cold flow model testing of an indirectly heated carbonate looping process. Chem Eng Technol 36:1479–1487. https://doi.org/10.1002/ceat.201300019

Junk M, Reitz M, Ströhle J, Epple B (2016) Technical and economical assessment of the indirectly heated carbonate looping process. J Energy Resour Technol 138:042210. https://doi.org/10.1115/1.4033142

Kremer J, Galloy A, Ströhle J, Epple B (2013) Continuous CO_2 capture in a 1-MW_{th} carbonate looping pilot plant. Chem Eng Technol 36:1518–1524. https://doi.org/10.1002/ceat.201300084

Kunii D, Levenspiel O (1991) Fluidization Engineering, 2nd edn. Butterworth-Heinemann, Boston

Lasheras A, Ströhle J, Galloy A, Epple B (2011) Carbonate looping process simulation using a 1D fluidized bed model for the carbonator. Int J Greenh Gas Control 5:686–693. https://doi.org/10.1016/j.ijggc.2011.01.005

Liu Z, Liu S, Shi R, Wang J, Xie M, Zheng S (2020) A control strategy of the air flow rate of coal-fired utility boilers based on the load demand. ACS Omega 5:31199–31208. https://doi.org/10.1021/acsomega.0c04585

Madejski P, Chmiel K, Subramanian N, Kuś T (2022) Methods and techniques for CO_2 capture: review of potential solutions and applications in modern energy technologies. Energies 15:887. https://doi.org/10.3390/en15030887

Magli F, Spinelli M, Fantini M, Romano MC, Gatti M (2022) Techno-economic optimization and off-design analysis of CO_2 purification units for cement plants with oxyfuel-based CO_2 capture. Int J Greenh Gas Control 115:103591. https://doi.org/10.1016/j.ijggc.2022.103591

Martínez I, Fernández JR, Abanades JC, Romano MC (2018) Integration of a fluidised bed Ca–Cu chemical looping process in a steel mill. Energy 163:570–584. https://doi.org/10.1016/j.energy.2018.08.123

Martínez I, Grasa G, Parkkinen J, Tynjälä T, Hyppänen T, Murillo R, Romano MC (2016) Review and research needs of Ca-looping systems modelling for post-combustion CO_2 capture applications. Int J Greenh Gas Control 50:271–304. https://doi.org/10.1016/j.ijggc.2016.04.002

Merk C, Grunau J, Riekhof M-C, Rickels W (2022) The need for local governance of global commons: the example of blue carbon ecosystems. Ecol Econ 201:107581. https://doi.org/10.1016/j.ecolecon.2022.107581

Mohn J, Szidat S, Fellner J, Rechberger H, Quartier R, Buchmann B, Emmenegger L (2008) Determination of biogenic and fossil CO_2 emitted by waste incineration based on $^{14}CO_2$ and mass balances. Bioresour Technol 99:6471–6479. https://doi.org/10.1016/j.biortech.2007.11.042

Mohn J, Szidat S, Zeyer K, Emmenegger L (2012) Fossil and biogenic CO_2 from waste incineration based on a yearlong radiocarbon study. Waste Manag 32:1516–1520. https://doi.org/10.1016/j.wasman.2012.04.002

Moora H, Roos I, Kask U, Kask L, Ounapuu K (2017) Determination of biomass content in combusted municipal waste and associated CO_2 emissions in Estonia. Energy Procedia 128:222–229. https://doi.org/10.1016/j.egypro.2017.09.059

Nhuchhen DR, Sit SP, Layzell DB (2022) Decarbonization of cement production in a hydrogen economy. Appl Energy 317:119180. https://doi.org/10.1016/j.apenergy.2022.119180

Obermoser M, Fellner J, Rechberger H (2009) Determination of reliable CO_2 emission factors for waste-to-energy plants. Waste Manag Res 27:907–913. https://doi.org/10.1177/0734242X09349763

Plaza MG, Martínez S, Rubiera F (2020) CO_2 capture, use, and storage in the cement industry: state of the art and expectations. Energies 13:5692. https://doi.org/10.3390/en13215692

Posch S, Haider M (2012) Optimization of CO_2 compression and purification units (CO_2CPU) for CCS power plants. Fuel 101:254–263. https://doi.org/10.1016/j.fuel.2011.07.039

Quader MA, Ahmed S (2017) Bioenergy with carbon capture and storage (BECCS). In: Rasul MG, Azad AK, Sharma SC (eds) Clean energy for sustainable development: comparisons and contrasts of new approaches. Academic Press, Amsterdam, Boston, Heidelberg, London, New York, Oxford, Paris, San Diego, San Francisco, Singapore, Sydney, Tokyo, pp 91–140

Reitz M, Junk M, Ströhle J, Epple B (2014) Design and erection of a 300 kW_{th} indirectly heated carbonate looping test facility. Energy Procedia 63:2170–2177. https://doi.org/10.1016/j.egypro.2014.11.236

Reitz M, Junk M, Ströhle J, Epple B (2016) Design and operation of a 300 kW_{th} indirectly heated carbonate looping pilot plant. Int J Greenh Gas Control 54:272–281. https://doi.org/10.1016/j.ijggc.2016.09.016

Rolfe A, Huang Y, Haaf M, Pita A, Rezvani S, Dave A, Hewitt NJ (2018) Technical and environmental study of calcium carbonate looping versus oxy-fuel options for low CO_2 emission cement plants. Int J Greenh Gas Control 75:85–97. https://doi.org/10.1016/j.ijggc.2018.05.020

Sarc R, Lorber KE (2013) Production, quality and quality assurance of refuse derived fuels (RDFs). Waste Manag 33:1825–1834. https://doi.org/10.1016/j.wasman.2013.05.004

Savage GM (1989) Thermal conductivity and specific heat of densified refuse derived fuel. Waste Manag Res 7:83–92. https://doi.org/10.1016/0734-242X(89)90010-4

Schorcht F, Kourti I, Scalet BM, Roudier S, Delgado Sancho L (2013) Best available techniques (BAT) reference document for the production of cement, lime and magnesium oxide: Industrial Emissions Directive 2010/75/EU (integrated pollution prevention and control). Publications Office, Luxembourg

Shimizu T, Hirama T, Hosoda H, Kitano K, Inagaki M, Tejima K (1999) A twin fluid-bed reactor for removal of CO_2 from combustion processes. Chem Eng Res Des 77:62–68. https://doi.org/10.1205/026387699525882

Spinelli M, Campanari S, Consonni S, Romano MC, Kreutz T, Ghezel-Ayagh H, Jolly S (2018) Molten carbonate fuel cells for retrofitting postcombustion CO_2 capture in coal and natural gas power plants. J Electrochem Energy Convers Storage 15:031001. https://doi.org/10.1115/1.4038601

Strezov V, Lucas JA, Evans TJ, Strezov L (2004) Effect of heating rate on the thermal properties and devolatilisation of coal. J Therm Anal Calorim 78:385–397. https://doi.org/10.1023/B:JTAN.0000046105.01273.61

Ströhle J, Hilz J, Epple B (2020) Performance of the carbonator and calciner during long-term carbonate looping tests in a 1 MW$_{th}$ pilot plant. J Environ Chem Eng 8:103578. https://doi.org/10.1016/j.jece.2019.103578

Ströhle J, Hofmann C, Greco-Coppi M, Epple B (2021) CO_2 capture from lime and cement plants using an indirectly heated carbonate looping process - the ANICA project. In: TCCS-11: CO_2 capture, transport and storage. Short papers from the 11th International Trondheim CCS Conference, Trondheim, Norway. June 21-23. SINTEF Academic Press, Oslo, pp 529–535

Ströhle J, Junk M, Kremer J, Galloy A, Epple B (2014) Carbonate looping experiments in a 1MW$_{th}$ pilot plant and model validation. Fuel 127:13–22. https://doi.org/10.1016/j.fuel.2013.12.043

Svensson E, Wiertzema H, Harvey S (2021) Potential for negative emissions by carbon capture and storage from a novel electric plasma calcination process for pulp and paper mills. Front Clim 3:705032. https://doi.org/10.3389/fclim.2021.705032

Velis CA, Longhurst PJ, Drew GH, Smith R, Pollard SJT (2010) Production and quality assurance of solid recovered fuels using mechanical—biological treatment (MBT) of waste: a comprehensive assessment. Crit Rev Environ Sci Technol 40:979–1105. https://doi.org/10.1080/10643380802586980

Voldsund M, Anantharaman R, Berstad D, De Lena E, Fu C, Gardarsdottir SO, Jamali A, Pérez-Calvo JF, Romano M, Roussanaly S, Ruppert J, Stallmann O, Sutter D (2019a) D4.6 CEMCAP comparative techno-economic analysis of CO_2 capture in cement plants

Voldsund M, Gardarsdottir S, De Lena E, Pérez-Calvo J-F, Jamali A, Berstad D, Fu C, Romano M, Roussanaly S, Anantharaman R, Hoppe H, Sutter D, Mazzotti M, Gazzani M, Cinti G, Jordal K (2019b) Comparison of technologies for CO_2 capture from cement production—part 1: technical evaluation. Energies 12:559. https://doi.org/10.3390/en12030559

Yang Y, Wang L, Xia D, Jiang Z, Jiang B, Zhang P (2020) Novel lime calcination system for CO_2 capture and its thermal-mass balance analysis. ACS Omega 5:27413–27424. https://doi.org/10.1021/acsomega.0c03850

Publisher's note Springer Nature remains neutral with regard to jurisdictional claims in published maps and institutional affiliations.

Authors and Affiliations

Martin Greco-Coppi[1] [ORCID] **· Carina Hofmann[1] · Diethelm Walter[2] · Jochen Ströhle[1]** [ORCID] **· Bernd Epple[1]** [ORCID]

✉   Martin Greco-Coppi
    martin.greco@est.tu-darmstadt.de

    Carina Hofmann
    carina.hofmann@est.tu-darmstadt.de

    Diethelm Walter
    diethelm.walter@lhoist.com

    Jochen Ströhle
    jochen.stroehle@est.tu-darmstadt.de

    Bernd Epple
    bernd.epple@est.tu-darmstadt.de

[1]   Technical University of Darmstadt, Institute for Energy Systems and Technology, Otto-Berndt-Str. 2, 64287 Darmstadt, Germany

[2]   Lhoist Germany Rheinkalk GmbH, Am Kalkstein 1, 42489 Wülfrath, Germany